Regulation of inside-out β1-integrin activation by CDCP1

Sara G. Pollan[1], **Fangjin Huang**[1], **Jamie M. Sperger**[2], **Joshua M. Lang**[2], **Colm Morrissey**[3], **Anne E. Cress**[4], **C. Y. Chu**[1], **Neil A. Bhowmick**[1], **Sungyong You**[1], **Michael R. Freeman**[1], **Danislav S. Spassov**[5], **Mark M. Moasser**[5], **William G. Carter**[6], **Shakti Ranjan Satapathy**[7], **Kavita Shah**[7], **Beatrice S. Knudsen**[1]

[1]Cedars-Sinai Medical Center, Los Angeles, CA 90048, USA

[2]University of Wisconsin School of Medicine and Public Health, Madison, WI 53705, USA

[3]University of Washington, Seattle, WA 98195, USA

[4]University of Arizona Cancer Center, Tucson, AZ 85704, USA

[5]University of California San Francisco, San Francisco, CA 94143, USA

[6]Fred Hutchinson Cancer Research Center, Seattle, WA 98109, USA

[7]Purdue University, West Lafayette, IN 47907, USA

Abstract

Tumor metastasis depends on the dynamic regulation of cell adhesion through β1-integrin. The Cub-Domain Containing Protein-1, CDCP1, is a transmembrane glycoprotein which regulates cell adhesion. Overexpression and loss of CDCP1 have been observed in the same cancer types to promote metastatic progression. Here, we demonstrate reduced CDCP1 expression in high-grade, primary prostate cancers, circulating tumor cells and tumor metastases of patients with castrate-resistant prostate cancer. CDCP1 is expressed in epithelial and not mesenchymal cells, and its cell surface and mRNA expression declines upon stimulation with TGFβ1 and epithelial-to-mesenchymal transition. Silencing of CDCP1 in DU145 and PC3 cells resulted in 3.4-fold higher proliferation of non-adherent cells and 4.4-fold greater anchorage independent growth. CDCP1-silenced tumors grew in 100% of mice, compared to 30% growth of CDCP1-expressing tumors. After CDCP1 silencing, cell adhesion and migration diminished 2.1-fold, caused by loss of inside-out activation of β1-integrin. We determined that the loss of CDCP1 reduces CDK5 kinase activity due to the phosphorylation of its regulatory subunit, CDK5R1/p35, by c-SRC on Y234. This generates a binding site for the C2 domain of PKCδ, which in turn phosphorylates CDK5 on T77.

The resulting dissociation of the CDK5R1/CDK5 complex abolishes the activity of CDK5. Mutations of CDK5-T77 and CDK5R1-Y234 phosphorylation sites re-establish the CDK5/CDKR1 complex and the inside-out activity of β1-integrin. Altogether, we discovered a new mechanism of regulation of CDK5 through loss of CDCP1, which dynamically regulates β1-integrin in non-adherent cells and which may promote vascular dissemination in patients with advanced prostate cancer.

Introduction

CDCP1 is a transmembrane cell surface receptor that is expressed in epithelial cells and regulates cell-cell and cell-matrix adhesion through complex formation with ITGB1/β1-integrin, tetraspanins, SRC, and PKCδ [1]. The major model system employed for studies of CDCP1 in prostate cancer is the androgen receptor negative prostate cancer line, PC3. CDCP1 was first identified as a tumor antigen on the surface of PC3 cells [2] and targeting it inhibited tumor metastasis in mice [3]. Function blocking antibodies inhibited CDCP1-triggered survival of PC3 cells during or soon after extravasation into the vasculature [4] and decreased metastatic colonization in the lungs [5]. Cleavage, phosphorylation, and glycosylation states of CDCP1 determine the extent of pro-metastatic activity and can in part be regulated by the androgen receptor [6]. An antibody preventing the cleavage of CDCP1 inhibited metastatic growth of PC3 cells [7, 8]. In addition to its intrinsic expression in PC3 cells, CDCP1 is also released from cells via extracellular vesicles where it is further processed [8–10].

When comparing data from multiple tumor types, both high CDCP1 expression and loss of CDCP1 expression have been described. In prostate cancer, staining intensities and subcellular localization differed in fresh frozen compared to formalin fixed and paraffin-embedded tissues. While CDCP1 expression was higher in frozen tumor compared to normal, the opposite was observed after tissue fixation. How the loss of function of CDCP1 triggers tumor metastasis is poorly understood. In a study of 100 patient tumors, the heterogeneity of CDCP1 expression levels across patient cancers and sensitivity to formalin fixation discouraged its development as a biomarker of aggressive tumor behavior [8]. While high expression of CDCP1 has been observed in PC3, no cell culture model exists to investigate the loss of CDCP1 in prostate cancer. The sole model available to investigate CDCP1 loss is an in vivo mouse model with CDCP1 knockout in mouse mammary tumor virus-driven tumors [11], which generates significantly larger mammary tumors. CDCP1 knockdown also enhances cell growth in response to EGF or heregulin stimulation and increases AKT and MAPK phosphorylation in cells that have lost adhesion [12].

CDCP1 phosphorylation leads to the sequestration of c-SRC and PKCδ, phosphorylation of PKCδ by c-SRC [13] and prevention of pro-apoptotic nuclear translocation of PKCδ [14]. The phosphorylation of CDCP1 is also regulated during the cell cycle. When cells detach during mitosis or after trypsinization in cell culture, CDCP1 is heavily phosphorylated by c-SRC [15]. While CDCP1 extracellular ligands have not been elucidated, the cleavage of CDCP1 in adherent cells by serine proteases [16] is associated with dimerization and movement into a detergent-resistant membrane domain [17]. In adherent prostate and breast

cancer cells, CDCP1 is required for the activation of ITGB1/β1-integrin and regulates clustering of ITGB1/β1-integrin outside of focal adhesions [6, 11, 18] and signaling to AKT [18]. Although CDCP1 and ITGB1/β1-integrin co-immunoprecipitate, the binding site between CDCP1 and ITGB1/β1-integrin has not been identified. ITGB1/β1-integrin is maintained in an "active" state, marked by extended extracellular domains with a ligand-binding site exposed that confers increased binding affinity for extra cellular matrix proteins. ITGB1/β1-integrin is usually activated from the outside-in through a conformational change that triggers its binding to Talin in the cytoplasm [19]. Talin bound to Integrin recruits kindlins, actin, vinculin, and focal adhesion kinase (FAK) to form a mature adhesion complex [20]. When cells detach, ITGB1/β1-integrin can be activated from the inside-out to prime cells for re-adhesion [21]. A few processes can lead to inside-out integrin activation [21–24] such as G protein subunit Gα13 and c-SRC binding directly to the cytoplasmic domain of ITGB1/β1-integrin or CDK5 kinase phosphorylating Talin which then binds and activates ITGB1/β1-integrin [25].

Examinations of patient tissue samples reveals that protein expression of cyclin-dependent kinase 5 (CDK5) and its regulatory subunit, CDK5R1/p35, are highly expressed in prostate cancer [26] and increase in expression when comparing metastatic to benign patient tissue samples [27]. CDK5R1/p35 localizes CDK5 to the membrane and cleavage of CDK5R1/p35 by calpain results in cytoplasmic and nuclear expression of p25/CDK5 [28]. CDK5 has been shown to regulate cell adhesion in epithelial cells [29] and keratinocytes [30] and treatment with a CDK5 inhibitor significantly reduced active ITGB1/β1-integrin expression [25]. Amplified CDK5 expression increases cell-matrix adhesion and migration [30] via clustering with Talin and ITGB1/β1-integrin during cell spreading [31]. Knockdown of CDK5 [25] prevents Talin phosphorylation on serine 425 and binding of TALIN to ITGB1/β1-integrin [32], demonstrating that CDK5 kinase activity is essential for inside-out activation of ITGB1/β1-integrin.

In this study, we demonstrated that the expression of CDCP1 is significantly decreased in a subgroup of aggressive prostate cancers. Using a model system of non-adherent cells, we identified a novel pathway that is initiated when CDCP1 expression is lost and that alters cell adhesion through reversible regulation of the inside-out activity of β1-integrin.

Results

Loss of CDCP1 expression in patients

To determine CDCP1 expression status during prostate cancer disease progression, we analyzed data from a large prostate cancer cohort $(n = 2115)$ [33], a tissue microarray (TMA) of lethal prostate cancer metastases [34], and a compendium of circulating tumor cells (CTCs) from patients with castration-resistant prostate cancer [35]. CDCP1 mRNA expression levels were compared between benign prostate ($n = 794$) and cases of Gleason Sum < 7 ($n = 328$), Gleason Sum = 7 ($n = 530$) and Gleason Sum > 7 (n = 203) prostate cancers (Fig. 1a). A significant decrease in average CDCP1 mRNA expression was observed between samples from prostate cancers with Gleason Sum > 7 compared to Gleason Sum = 7.

Since cancers with Gleason Sum > 7 metastasize more frequently, we performed an immunohistochemical analysis of CDCP1 expression in a TMA displaying multiple metastatic sites ($n = 178$) from 44 patients who succumbed to prostate cancer. CDCP1 protein expression was scored in the cytoplasm and membrane (Supplementary Fig. 1A). In order to compare protein and mRNA expression of CDCP1, we determined the correlation in LuCaP xenografts [36]. The correlation of CDCP1 protein and mRNA expression was high ($r = 0.74$) (Supplementary Fig. 1B). Since CDCP1 is actively internalized and removed from the cell surface [8], expression of CDCP1 in the TMA was evaluated in the cytoplasm and on the cell surface in normal prostate epithelium, primary, and metastatic tumors (Fig. 1b). CDCP1 expression was only observed in epithelial cells and not in other cell types. Compared to normal epithelium, CDCP1 membrane expression significantly declined ($p < 0.05$) in primary prostate cancer. In contrast, cytoplasmic expression did not change significantly. However, in metastatic compared to primary tumors, CDCP1 expression was lower in all subcellular compartments (Fig. 1b). While in these cases of lethal prostate cancer metastasis the average CDCP1 protein expression was markedly reduced, some patient cancers demonstrated high CDCP1 expression. These results demonstrate that the greatest loss of CDCP1 occurs in the transition from primary to metastatic tumors; however, loss of CDCP1 expression is heterogeneous among tumors.

CTCs are representative of cancer cells that metastasize to distant sites. To determine whether tumor cells with reduced CDCP1 expression are detectable in the circulation, we analyzed CDCP1 mRNA expression in CTCs from patients with advanced, castration-resistant prostate cancer isolated through the VERSA microfluidic system [35] (Fig. 1c). mRNA was isolated from pooled CTCs, which were captured from nine patients using an antibody to EpCAM. One patient demonstrated CDCP1 expression at the limit of detection and in two patients CDCP1 mRNA levels were above the limit of detection. CDCP1-positive samples were also positive for PSA and for the epithelial-specific EpCam, while CDCP1-negative cells lacked these markers. The observation that CTCs isolated with EpCam antibodies may not express a sufficient amount of EpCam RNA for detection by qPCR has been previously observed [37]. The prostate cancer origin of all CTCs was confirmed through expression of AR in all samples. The small amount of lymphocyte contamination did not affect CDCP1 mRNA measurements, since lymphocytes do not express CDCP1 [38]. Collectively, CDCP1 mRNA expression in CTCs was highest in cells positive for epithelial markers, such as cytokeratin (Krt8) and EpCam.

Since in our studies CDCP1 mRNA expression was associated with epithelial differentiation in CTCs, we investigated a possible connection between the loss of CDCP1, epithelial-to-mesenchymal transition (EMT), and TGFβ1. We analyzed 260 cases of metastatic prostate cancer [33] (Fig. 1d). Genes differentially expressed in CDCP1 high vs. low-expressing tumors were ranked according to the results of the *t*-test. We then calculated the normalized gene set enrichment score (GSEA) of the hallmark EMT gene signature [39, 40] within differentially expressed genes. The normalized enrichment score was −1.73 (NES = −1.73, FDR = 0.004), attributable to the high expression of mesenchymal genes in the CDCP1 low group (Supplementary Fig. 2). A heatmap of expression levels of individual genes at the leading edge of the enrichment demonstrates high expression of mesenchymal genes in most of the cases within the CDCP1 low group compared /to the CDCP1 high group (Fig. 1d).

Loss of CDCP1 is stimulated by TGFβ1 treatment

In contrast to our data in human tissues, higher levels of CDCP1 expression have been reported in mesenchymal ARCaPM prostate cancer cells vs. epithelial ARCaPE cells [8], warranting a more detailed investigation of the association between CDCP1 and EMT. Therefore, we investigated whether the loss of CDCP1 can be caused directly by TGFβ1, a strong inducer of EMT. To this point, we analyzed the enrichment of a hallmark TGFβ1 signaling signature in metastatic prostate cancers from patients. The TGFβ1 signaling signature was enriched in cases with low, but not with high CDCP1 expression (NES = −1.2, FDR = 0.178) (Fig. 2a). Based on this result, we determined whether TGFβ1 treatment of DU145 and PC3 prostate cancer cells reduces CDCP1 expression. We quantified the surface expression of full-length CDCP1 by fluorescence-activated cell sorting (FACS) analysis in E-cadherin-positive (E+) cells (Fig. 2b–d). 29.4% of PC3-E+ cells and 18.1% of DU145-E+ cells expressed the full-length form of CDCP1 on the cell surface (Fig. 2b, Supplementary Fig. 3A). After treatment of PC3 and DU145 cell lines with TGFβ1 for 4 days, full-length CDCP1 was no longer expressed on the cell surface (Fig. 2c). The kinetics of regulation of CDCP1 expression by TGFβ1 were investigated in a 7-day time course. TGFβ1 treatment for 4 days greatly diminished the cell surface expression of E-cadherin and CDCP1 and removal of TGFβ1 led to rapid re-expression of CDCP1 to pretreatment levels (Fig. 2c–d, Supplementary Fig. 3B–D). The amount of CDCP1 surface expression measured by FACS analysis (Fig. 2c) and membrane expression measured by Western blotting of the membrane fraction (Supplementary Fig. 3D) corresponds to total CDCP1 mRNA expression (Fig. 2d). This data demonstrates that in DU145 cells, exposure to TGFβ1 leads to loss of both E-cadherin and CDCP1. The loss of both surface membrane proteins is reversible after removal of TGFβ1.

Changes in growth and adhesion of tumor cells after loss of CDCP1

Next, we questioned the functional consequences of reduced CDCP1 expression in E-cadherin-negative (E−) DU145 and PC3 cells. CDCP1 was silenced using previously published short hairpins [11]. Lentiviral transfection of the short hairpins resulted in robust loss of CDCP1 protein expression in both DU145 and PC3 cells (Supplementary Fig. 4A). Since we observed the loss of CDCP1 in CTCs and since CDCP1 silencing is published to change the phosphorylation of FAK in suspension [41], we investigated growth in suspension of E⁻DU145 and E⁻PC3 cells after silencing of CDCP1. CDCP1 knockdown cells were released from tissue culture plates with 5 mM EDTA and cultured in suspension on HEMA-coated plates. After 24 h in suspension (Supplementary Fig. 4B), the growth of DU145/shCDCP1 and PC3/shCDCP1 was increased 3.4-fold compared to control cells (Fig. 3a, Supplementary Fig. 4C). Growth of DU145/shCDCP1 in suspension was comparable to growth under adherent conditions (Supplementary Fig. 4C). We also employed a colony formation assay in soft agar to evaluate changes in anchorage independent growth after loss of CDCP1. In this assay, 4.4-fold more colonies were observed in CDCP1-silenced cells compared to controls (Fig. 3b). In addition to the increase in colony numbers, colony size was also increased. Next, we evaluated the consequences of CDCP1 loss in subcutaneous cell line xenografts in mice *(n = 10 per group)*. As expected, after 9 weeks the growth of E⁻DU145/shControl cells in mice was poor [36]. Only three xenografts were recovered from 10 injections. In contrast 10 tumors grew after injection of CDCP1-silenced tumor cells.

Average tumor volume was 800 mm^3 in mice that received subcutaneous DU145/shCDCP1 compared to an average tumor volume of 50 mm^3 in mice that received control cells (Fig. 3c, Supplementary Fig. 5A, B).

Under regular in vitro culture conditions, there was no difference in morphology between control and DU145/shCDCP1 cells (Supplementary Fig. 4B). However, upon adhesion of DU145/shCDCP1 cells that were kept in suspension for 2 h, we observed an 82% reduction in adhesion relative to control cells. Lower rates of adhesion were observed to plates coated with Matrigel, collagen-I, and fibronectin (Fig. 3c). In addition, the decreased cell adhesion resulted in reduced cell migration in a Transwell migration assay (Fig. 3d). Collectively these data demonstrate that CDCP1 loss decreases cell adhesion and migration, but increases the growth of tumor cells under conditions of weak or no adhesion.

Inside-out activity of ITGB1/β1-integrin is reduced in CDCP1-silenced cells

As a next step, we investigated the mechanism leading to the decrease in cell adhesion. Based on published data, CDCP1 immunoprecipitates with ITGB1/β1-integrin [18]. We employed the well-characterized HUTS-4 antibody, which specifically reacts with the active form of ITGB1/β1-integrin to investigate the effect of CDCP1 loss on inside-out activation of ITGB1/β1-integrin in non-adherent cells. The amount of HUTS-4 antibody binding was determined in CDCP1-silenced, adherent cells or shCDCP1 cells suspended for 3 h on HEMA-coated plated before analysis by immunocytochemistry/immunofluorescence (ICC/IF), FACS, or western blotting (Fig. 4a–e). In contrast to adherent cells, HUTS-4 binding to suspended cells was below the limit of detection after silencing of CDCP1 while total ITGB1/p1-integrin levels were unchanged. In homogenized xenografts of CDCP1-silenced DU145 cells, the activation of ITGB1/β1-integrin was also significantly reduced (Fig. 4e). FACS analysis and western blotting further confirmed the inactivation of ITGB1/β1-integrin in all suspended DU145/shCDCP1 compared to control, CDCP1-positive cells (Fig. 4a, b). The active state of ITGB1/β1-integrin was lost after 10 min in suspension (Fig. 4c). Interestingly, suspension of DU145/shCDCP1 resulted in phosphorylation of SRC on Y416 (Fig. 4d). Collectively, these data demonstrate that CDCP1 expression regulates the inside-out activation of ITGB1/β1-integrin in nonadherent cells. In contrast, steady state activation of ITGB1/β1-integrin in adherent cells, which is caused by outside-in activation [42], is not sensitive to loss of CDCP1 in DU145 and PC3 cells.

Loss of CDCP1 leads to phosphorylation of CDK5R1/p35 and inhibition of CDK5 kinase

One of the mechanisms that is known to regulate inside-out activation of ITGB1/β1-integrin is the binding of TALIN to the cytoplasmic tail of ITGB1/β1-integrin [42]. In this context, TALIN is phosphorylated on S425 by CDK5 [25]. Therefore, we questioned whether CDCP1 silencing reduces the activity of CDK5. This can occur by preventing binding of the CDK5 catalytic subunit to the regulatory subunit, CDK5R1/p35 [25, 43]. First, we determined CDK5 activity in a CDK5 kinase assay [44]. The phosphorylation of exogenous CDK5 substrate was significantly lower in DU145/shCDCP1 compared to control cells (Supplementary Fig. 6A). Next, we measured the formation of CDK5-CDK5R1 complexes through co-immunoprecipitation (Fig. 5a, b). Upon CDCP1 silencing, CDK5R1/p35 dissociated from CDK5 as demonstrated by reciprocal co-immunoprecipitation experiments

(Fig. 5a). In addition, the CDK5R1-CDK5-pTALIN-ITGB1 complex was disrupted in CDCP1-silenced cells (Fig. 5b) such that CDK5 remains bound to TALIN in CDCP1-silenced cells while CDK5R1 is absent from the complex (Supplementary Fig. 6B).

Next, we hypothesized that the activation of c-SRC leads to dissociation of the CDK5R1-CDK5 complex. Since the loss of CDCP1 results in the removal of the major cell surface anchor of c-SRC, c-SRC sequestration to the plasma membrane is reduced and c-SRC is directed to different substrates [45]. Therefore, we questioned whether c-SRC might phosphorylate either CDK5 or CDK5R1/p35 to cause the dissociation of the CDK5-CDK5R1 complex. In order to determine whether CDK5 or CDK5R1/p35 are phosphorylated by c-SRC, we precipitated both proteins in DU145/shCDCP1 cells. While we did not observe CDK5 phosphorylation, c-SRC protein was detected in CDK5R1/p35 immunoprecipitates (Supplementary Fig. 6C). To determine phosphorylation by c-SRC within the complex, we probed the CDK5R1/p35 immunoprecipitates with the global anti-phosphotyrosine antibody, 4G10 (Fig. 5c). Interestingly, three 4G10-reactive bands appeared in the western blot. Reprobing assigned these bands to CDK5R1/p35, SRC, and PKCδ. These data demonstrate that PKCδ like c-SRC is redirected to new complexes in CDCP1-silenced cells, since it is also no longer sequestered by CDCP1 [46]. Further, the loss of CDCP1 can lead to increased c-SRC activation and redirection of c-SRC to a novel substrate, CDK5R1/p35. Based on this data, we postulated that inhibiting c-SRC with Saracatinib should reverse the inactivation of CDK5 and lead to phosphorylation of TALIN on S425. Therefore, we employed TALIN phosphorylation as a direct readout of CDK5 kinase activity [25]. As we predicted, Saracatinib treatment of CDCP1-silenced cells re-established TALIN-S425 phosphorylation and inside-out activity of ITGB1/β1-integrin measured by HUTS-4 (Fig. 5d).

In CDCP1-silenced, adherent cells, TALIN was phosphorylated and ITGB1/β1-integrin was in an active state (Fig. 4d). Therefore, we postulated that the outside-in activation of ITGB1/β1-integrin occurring upon cell adhesion leads to the steady-state activation of CDK5 activity. This would require de-phosphorylation of CDK5R1/p35 in CDCP1-silenced cells to re-establish the CDK5-CDK5R1 complex. Therefore, we tested the effects of Na-Vanadate on CDK5R1/p35 phosphorylation. Treatment of suspended cells with Vanadate delayed cell adhesion to cell culture plates. After 15 min, there was a 3.5-fold reduction in the number of adherent cells in Na-Vanadate-treated compared to control cultures (Fig. 5e). In addition, the integrity of the CDK5R1/p35 complex and phosphorylation of proteins was maintained in the Na-Vanadate-treated cells (Fig. 5f).

Role of PKCδ in the regulation of CDK5 activity

Since we detected PKCδ in CDK5R1/p35 immunoprecipitates, we questioned whether PKCδ is involved in the regulation of inside-out ITGB1/β1-integrin activity. To address this point, PKCδ was silenced in DU145/shCDCP1 or control cells (Fig. 6a). As expected, DU145/shCDCP1 cells did not express active ITGB1/β1-integrin. Silencing of PKCδ, but not expression of a scrambled control oligonucleotide, accompanied ITGB1/β1-integrin activation. The level of ITGB1/β1-integrin activity in DU145/shCDCP1/siPKCδ equaled that of DU145 cells expressing CDCP1. Silencing PKCδ in parent, CDCP1-expressing cells

did not change the activation of ITGB1/β1-integrin. In addition, and as expected, TALIN phosphorylation on S425 paralleled ITGB1/β1-integrin activity after PKCδ knockdown, suggesting regulation of CDK5 through silencing of PKCδ (Fig. 6a).

Since the C2 domain of PKCδ binds to a SRC phosphorylation motif in CDCP1 [47], we determined whether the PKCδ-C2 domain is responsible for binding to CDK5R1/p35. Therefore, we expressed GFP fused to the C2 domain of PKCδ in DU145/shCDCP1 cells (Fig. 6b). Expression of the C2 domain prevented binding of endogenous PKCδ and re-established the complex between CDK5 and CDK5R1/p35. Consequently, inside-out activation of ITGB1/β1-integrin was detectable in a western blot. In contrast, in cells expressing the empty vector, the endogenous PKCδ bound to CDK5R1/p35 and in these cells, CDK5R1-CDK5 complex formation and ITGB1/β1-integrin activation were inhibited (Fig. 6b).

A kinase assay was used to confirm increased CDK5 kinase activity by expression of the PKCδ-C2 domain (Fig. 6c). We compared CDK5 kinase activity in DU145/shCDCP1cells expressing GFP-PKCδ-C2 with DU145/shCDCP1 and DU145/shControl cells expressing the empty vector with GFP. In cells expressing the PKCδ-C2 domain, the activity of CDK5 was increased by 2.7-fold compared to DU145/shCDCP1 cells. These data show that endogenous PKCδ binds CDK5R1/p35 via the C2 domain and that the binding decreases CDK5 kinase activity.

Phosphorylation of CDK5-T77 by PKCδ inhibits CDK5 kinase activity

In order to determine if PKCδ kinase activity is necessary for dissociation of the CDK5-CDK5R1 complex, we expressed a GFP-fusion protein of inactive PKCδ. The K376R mutation in the kinase domain of PKCδ abolishes its catalytic activity [48] (Fig. 6d). Forced expression of this kinase inactive mutant (GFP-PKCδ-KD) resulted in co-precipitation with CDK5R1/p35. Interestingly, while GFP-PKCδ-KD was detected by anti-GFP antibodies, it did not react with antibodies against the PKCδ-C2 domain. Results demonstrated that binding of PKCδ-KD to CDK5R1/p35 prevented binding of endogenous PKCδ and led to complex formation between CDK5 and CDK5R1/p35. As expected, ITGB1/β1-integrin was active in DU145/shCDCP1-expressing PKCδ-KD. To further confirm that PKCδ kinase activity causes dissociation of CDK5R1/p35 and CDK5, we treated cells with 10 nM Go6983, an inhibitor that blocks multiple PKC kinases. Treatment with Go6983 during culture of DU145/shCDCP1 on HEMA-coated plates re-established the CDK5-CDK5R1 complex (Fig. 6e). Collectively, these results demonstrate that PKCδ binds CDK5R1/p35 via its C2 domain and that dissociation of CDK5R1/p35 from CDK5 requires the PKCδ kinase domain.

To further characterize the interactions of PKCδ with p-CDK5R1/p35, we generated mutations in candidate c-SRC substrate phosphorylation sequences within CDK5R1/p35. Two of the mutants, CDK5R1-Y231F and CDK5R1-Y234F, were expressed with a MYC tag. After 3 h suspension on HEMA-coated plates, a MYC pulldown revealed that CDK5 was able to complex with CDK5R1-Y234F, but not CDK5R1-Y231F (Fig. 6f). This result demonstrates that after its phosphorylation by c-SRC, Tyr234 serves as the binding site for PKCδ. To determine whether the C2 domain of PKCδ is critical for PKCδ binding to

CDK5R1-Y234, we co-transfected DU145/shCDCP1 cells with MYC-CDK5R1 mutants and GFP-PKCδ-C2 (Fig. 6f). As predicted, GFP-PKCδ-C2 bound MYC-CDK5R1-wt and MYC-CDK5R1-Y231F mutant, but not MYC-CDK5R1-Y234F. Consistent with these results, ITGB1/β1-integrin activation occurred only in cells expressing MYC-CDK5R1-Y234F, but not in wild-type or MYC-CDK5R1-Y231F-expressing cells. Altogether, these date demonstrate that PKCδ binds CDK5R1-pY234 via the C2 domain.

Next, we characterized PKCδ phosphorylation of the CDK5-CDK5R1 complex by identifying potential target sequences that might be phosphorylated by PKCδ in CDK5 or CDK5R1/p35 (Fig. 7). We predicted that mutating these PKCδ phosphorylation sites would prevent the dissociation of CDK5 from CDKR1 and lead to inside out activation of ITGB1/β1-integrin. Indeed, CDK5-T77A fit this prediction. The MYC-CDK5-T77A mutant formed a complex with CDK5R1/p35, but the wt-MYC-CDK5 did not (Fig. 7a). In addition, MYC-CDK5-T77A co-precipitated with active ITGB1/β1-integrin and resulted in staining with HUTS-4 in 78% of cells (Fig. 7b). Finally, we wanted to determine whether c-SRC-pY416 or PKCδ are present in the CDK5R1-CDK5-T77A complex. We probed the MYC-CDK5-T77A immunoprecipitated complexes with SRC-pY417 and PKCδ reactive antibodies. There were no bands corresponding to these proteins in the western blots (Fig. 7a). However, when total CDK5R1/p35, which consists of complexed and uncomplexed protein, was precipitated from CDK5-T77A-expressing cells, Src-pY416 and PKCδ were detected in the immunoprecipitates (Fig. 7c). In addition, the immunoprecipitate also contained CDK5-T77A. From these data we infer that CDK5R1/p35 exists in two compartments in the CDK5-T77A-expressing cells. One population of CDK5R1/p35 is bound to CDK5-T77A and does not bind c-SRC-pY416 or PKCδ. The other population of CDK5R1/p35 is complexed to c-SRC-pY416 and PKCδ, but does not bind CDK5-T77A.

In contrast to CDK5-T77A, the T77D mutant is predicted to mimic CDK5-T77 phosphorylated by PKCδ and lead to inhibition of ITGB1/β1-integrin activation. To test this hypothesis, we expressed a MYC-CDK5-T77D in DU145 cells expressing CDCP1 and active ITGB1/β1-integrin (Fig. 7d). Immunoprecipitation of MYC-CDK5-T77D using an antibody to the MYC-tag demonstrated decreased binding of total as well as active ITGB1/β1-integrin compared to MYC-CDK5-wt. However, a similar amount of CDK5R1/p35 precipitated with MYC-CDK5-wt and MYC-CDK5-T77D, suggesting that the T77D mutation does not alter binding to CDK5R1/p35 and that CDK5 is inactive despite binding to CDK5R1/p35. The western blot results of ITGB1/β1-integrin inactivation in cells expressing CDK5-T77D were confirmed by immunofluorescent staining (Fig. 7b), demonstrating a 5-fold loss of HUTS-4 staining in CDK5-T77D compared to CDK5-wt or CDK5-T77A mutant. Collectively, these results demonstrate that CDK5-T77D and likely CDK5-T77 phosphorylation by PKCδ diminishes CDK5 kinase activity, but does not interfere with CDK5-CDK5R1 complex formation.

Discussion

In this study, we describe a novel, dynamic, and reversible mechanism that regulates inside-out activation of ITGB1/β1-integrin (Fig. 8). We demonstrate, in a model system of non-adherent tumor cells, that the loss of the cell surface receptor CDCP1 initiates a signaling

cascade that leads to inactivation of β1-integrin. The translational relevance of this mechanism is supported by a significant reduction of CDCP1 expression in high-grade primary prostate cancer, CTCs, and tumor metastasis in patients with castrate- resistant prostate cancer. Exposure of adherent prostate cancer cells to TGFβ1 rapidly inhibited mRNA and surface protein expression of CDCP1 with kinetics similar to E-cadherin. Upon losing CDCP1 expression, cells exhibit 3.4-fold higher proliferation rates in suspension, a 4.4-fold increase of anchorage-independent colony formation, and the ability for rapid in vivo growth as xenografts in mice. However, CDCP1 loss causes a 2.1-fold reduction in cell adhesion and migration. Consistent with the adhesion deficit, inside-out activity of β1-integrin is reduced in non-adherent DU145 and PC3 cells. The mechanism responsible for inactivation of βi-integrin entails de novo phosphorylation of CDK5R1/p35 by c-SRC on CDK5R1-Y234 and binding of PKCδ to this phosphosite via its C2 domain. PKCδ phosphorylates CDK5-T77, leading to dissociation of CDK5R1/p35 from CDK5 and inactivation of CDK5 kinase. Consequently, and as demonstrated previously [25], phosphorylation of TALIN by CDK5 that is necessary for inside-out β1-integrin activity, is abrogated. The phosphorylation of CDK5R1/p35 is reversed upon cell adhesion, and the duration of β1-integrin inactivation can be enhanced through treatment of cells with phosphatase inhibitors. Altogether, this novel mechanism regulates the dynamics of cell adhesion and reduces adhesion of tumor cells at specific steps of the metastatic cascade, for example, during vascular intravasation. The loss of CDCP1 expression in patient prostate cancers is consistent with an increased efficiency of metastatic dissemination of CDCP1-negative tumor cells.

The loss of CDCP1 changes the spectrum of SRC substrate phosphorylation. In suspended cells, CDCP1 is one of the main proteins that is phosphorylated on tyrosine [49, 50] and c-SRC and PKCδ are its key binding partners [51]. Upon phosphorylation of CDCP1 on Tyr734, c-SRC binds via its SH2 domain and further phosphorylates CDCP1 on Tyr762 to create a binding site for the PKCδ-C2 domain [52]. Under these circumstances, CDCP1 negatively regulates c-SRC and PKCδ [53] by sequestering the kinases away from their substrates. For example, c-SRC binding to CDCP1 prevents SRC phosphorylation of GAP-junction proteins [54] and FAK [45], and thereby reduces the oncogenic activity of SRC [15]. Upon loss of CDCP1, c-SRC and PKCδ are freed to bind to new substrates. We identified a novel SRC substrate, CDK5R1/p35, that is phosphorylated on Tyr234 in CDCP1 deficient, nonadherent cells. As is the case for CDCP1, phosphorylation of CDK5R1/p35 by c-SRC generates a binding site for the PKCδ-C2 domain. While we demonstrate de novo phosphorylation of CDK5R1/p35 in CDCP1-silenced cells, it is unclear whether there are additional protein complexes formed through coordination of c-SRC and PKCδ phosphorylation that are responsible for metastatic dissemination of CDCP1-negative cancer cells.

The reversible assembly of CDK5-CDK5R1 complexes in CDCP1-deficient cells is regulated through kinetics of protein phosphorylation and/or protein-protein interactions. CDK5 activity requires binding of its regulatory subunit, CDK5R1/p35. In CDCP1-negative cells, the first reaction promoting inactivation of CDK5 is the phosphorylation of CDK5R1/p35 by c-SRC and the binding of PKCδ to CDK5R1/p35. PKCδ phosphorylates CDK5 in the kinase domain, which inhibits the kinase activity. It is not known if binding via

the C2 domain is sufficient to fully activate the PKCδ kinase, or if additional changes are needed through lipid and Ca2+ binding to the PKCδ-C1 domain. Our data demonstrating that CDK5 activity is re-established after expression of kinase-inactive PKCδ or the PKCδ C2 domain can simply be explained by the competition with endogenous PKCδ. However, the final CDK5R1-CDK5 complex does not include PKCδ (Fig. 7c), suggesting that PKCδ binding may disadvantage CDK5R1-CDK5 complex formation. It is possible that conformational changes in the PKCδ C2 domain may contribute to the dissociation of PKCδ from CDK5R1/p35. It is known that the ON/OFF state of PKCδ kinase activity and possibly also the engagement of the PKCδ kinase domain with its substrate regulates the structure of the C2 domain. We confirmed previously published data that mutational inactivation of the PKCδ kinase changes the conformation of the PKCδ-C2 domain [55] such that the antibody reactive with the PKCδ- C2 domain does not bind to mutationally inactivated PKCδ or PKCδ after inhibition by Go6983 (Fig. 6d). This conformational change affecting the C2 domain did not interfere with the binding of PKCδ to CDK5R1/p35. However, our data is consistent with a model that engaging the PKCδ kinase loosens the binding between the C2 domain and CDK5R1-pY234, such that pY234 can become dephosphorylated. In support of this hypothesis, treatment with Vanadate delayed cell adhesion by preventing dephosphorylation of CDK5R1/p35 (Fig. 5f). Ultimately, phosphorylation of CDK5 by PKCδ and CDK5 dissociation from CDK5R1/p35 could provide a novel mechanism, which promotes the nuclear translocation of CDK5 [56].

Another question that arises from our results is how individual steps in the CDK5R1-β1-integrin pathway, initiated through the loss of CDCP1, promote tumor metastasis. Most published literature examines mechanisms of tumor metastasis that are triggered by overexpression of CDCP1 (reviewed in [57]), activation of PKCδ [58] and CDK5 [59], and increased β1-integrin expression [60]. However, a number of studies report that the loss of CDCP1 in primary and metastatic tumors, specifically in prostate [61], breast [11, 61], colorectal [61, 62], endometroid [63], and esophageal squamous [64] cancers, is associated with growth and metastasis. At first glance, loss of CDCP1 would be expected to decrease metastatic dissemination of cancer cells [65] through inactivation of β1-integrin. However, the intuitive concept that reducing cell adhesion antagonizes metastatic progression has been challenged by reports of enhanced metastatic ability by cancer cells expressing β1-integrin mutants with defective inside-out activation [66]. It is possible that in these cancers transitions in the metastatic cascade that require detachment from the ECM are major bottlenecks of metastatic progression, which can be overcome through weakening β1-integrin- mediated adhesion.

Tumors expressing low CDCP1 levels might require a different treatment strategy when considering pharmacological targeting of c-SRC and PKCδ. We demonstrated that in CDCP1-negative cells, the inhibition of these kinases induces inside-out activation of β1-integrin, which might accelerate tumor metastasis. For example, Dasatinib, a potent inhibitor of c-SRC has not met the expected efficacy in metastatic prostate cancer [67] perhaps because patients were stratified for treatment based on presumed c-SRC kinase activity and not based on the specificity of c-SRC substrate phosphorylation. Inhibition of β1-integrin and several α-integrin subunits through humanized antibodies bears therapeutic promise as anti-cancer drugs [68, 69]. However, the efficacy of this treatment might be reduced in

cancers with inactive β1-integrin in CTCs and patients could be stratified prior to treatment based on CDCP1 expression in CTCs.

Treatment with PKCδ inhibitors might also require careful patient selection, since mutations causing loss of function of PKCδ have been observed in multiple tumor types [70]. Consistent with the concept of a tumor suppressive function of PKCδ, phosphorylation by c-SRC leads to a loss of PKC8's pro-apoptotic activity in the nucleus and promotes the survival of tumor cells [71]. In contrast to inhibition of PKCδ kinase activity in the CDCP1 complex [53, 71], the activity of PKCδ is maintained in the CDK5R1/p35 complex. After binding to CDK5R1/p35, PKCδ becomes phosphorylated on tyrosine as detected by 4G10, an antibody that preferentially binds to phosphotyrosines after their phosphorylation by SRC kinases [72]. However, it is unclear whether phosphorylation occurs at PKCδ-Y311 [71], or perhaps on a different tyrosine, which does not diminish the kinase activity of PKCδ. Finally, while inhibiting CDK5 might reduce metastatic progression in tumors with overexpression of CDCP1, the response to CDK5 inhibitors may be diminished in tumors that lack CDCP1 expression, and patients with such tumors would be unnecessarily exposed to drug toxicity. Thus, it will be important to screen patients' tumor cells for loss of CDCP1 in order to select the appropriate anti-metastatic drug treatments.

A limitation of our study is that we have not demonstrated that the loss of β1-integrin inside-out activity is the sole reason for metastatic progression of CDCP1-negative tumor cells. In addition to the adhesion defect caused by the loss of CDCP1, there is constitutive activation of FAK in CDCP1-negative cells [41]. The activation of FAK in non-adherent cells is a major mechanism of anoikis resistance (reviewed in [73]). Further, in a CDCP1-knockout mouse breast cancer model, tumor formation in vivo was enhanced and exhibited increased FAK activity [15]. In agreement with these observations, in our cell suspension system, FAK is constitutively active despite inactivation of β1-integrin (data not shown). This is consistent with an uncoupling between FAK activation and β1-integrin. How FAK becomes activated in cells that express inactive β1-integrin is not known. It is also unclear whether constitutive activation of endogenous FAK in CDCP1-negative cells by itself accounts for the observed selection of cancer cells with reduced CDCP1 expression in patient tumors. Therefore, future research is needed to investigate the activation of additional pathways after CDCP1 loss and their individual roles in prostate cancer progression with the ultimate goal to deliver individualized anti-metastatic drug treatments to patients with advanced prostate cancer.

Materials and methods

Antibodies

The following antibodies were purchased from Cell Signaling Technologies (3 Trask Lane, Danvers, MA, 01923): E-cadherin (24E10) Rabbit mAb #3195, Rabbit anti-human CDCP1 (#4115), β1-integrin (#4706), Phospho-Talin (Ser425) (#13589), Talin (#4021), B-Actin (8H10D10) Mouse mAb (#3700), CDK5R1/p35 (#2680), CDK5 (#12134), Phospho-SRC (#2101), SRC (#2108), PKCδ (#2058), Phospho-FAK (#3284), FAK (#13009), Myc-Tag (9B11) Mouse mAb #2276.

Anti-phospho-tyrosine antibody, clone 4G10 (05–321) and activated β1-integrin (HUTS4, MAB2079Z) were obtained from Millipore (400 Summit Drive, Burlington, MA, 01803). F(ab ')2-Goat anti-Mouse IgG (H+L) Secondary Antibody, Alexa Fluor® 555 conjugate (A-21425), F (ab ')2-Goat anti-Rabbit IgG (H+L) Secondary Antibody, Alexa Fluor® 488 conjugate (A-11070), F(ab ')2-Goat anti-Mouse IgG (H+L) Secondary Antibody, Alexa Fluor® 488 conjugate (A-11017) and F(ab ')2-Goat anti-Rabbit IgG (H +L) Secondary Antibody, Alexa Fluor 594 conjugate (A- 11072) were purchased from Life Technologies (5791 Van Allen Way, Carlsbad, CA, 92008). Anti-Sodium Potassium ATPase antibody [EP1845Y] ab76020 was purchased from Abcam (1 Kendall Square, Suite B2304, Cambridge, MA, 02139).

Gö 6983 (#G1918) was purchased from Sigma-Aldrich (3300S 2nd St, St. Louis, MO, 63118). Saracatinib (#S1006) was purchased from Selleckchem (9330 Kirby Drive, STE 200, Houston, TX, 77054). All experiments were conducted with three technical and two biological replicates.

Cell lines

E-cadherin-positive and negative DU145 and PC3 cells were previously described by our group [36]. Briefly, parent DU145 cells were sorted using FACS based on E-cadherin expression. Cells with the lowest 10% and highest 10% E-cadherin expression were placed in three-dimensional Matrigel, and resulting colonies were picked individually and propagated in two dimensions. The DU145 sublines are stable populations of epithelial DU145 (E$^+$DU145/T-DU145) and mesenchymal DU145 (E$^−$DU145/S-DU145). Cell lines were recently authenticated as DU145 or PC3 cells by short tandem repeat profiling and tested free of mycoplasma contamination (University of Arizona Genetics Core).

TGFβI stimulation and qPCR

Cell lines were treated with 10ng/mL TGFβ1 for 4–6 days with daily replacement of TGFβ1. For the time course, E$^+$ and E$^-$DU145 and PC-3 cells were treated with 10ng/mL TGFβ1 for 4 days and then cells were washed twice with PBS and full media was given without TGFβ1 treatment for days 5–7. SYBR qPCR with validated primers for CDCP1 Fw: 5 '-TGTCCATCAAGTCTGGAGAAAGA-3 '; Rv: 5 '-TGAAGCTGAACCTCCCCAAAA-3 '.

Fluorescence-activated cell sorting

EDU145/shControl and shCDCP1 were dissociated with EDTA and suspended in HEMA-coated 60 mM tissue culture plates for 3 h. 1×10^6 cells were fixed for 10 min with 3.4% paraformaldehyde (PFA). Cells were spun at $1000 \times g$ for 2 min and re-suspended in 1:1000 primary antibodies in 5% goat serum in PBS for 1 h. Cells were washed with PBS, then incubated with 1:2000 secondary antibodies in 5% goat serum in PBS for 30 min. Cells were washed, re-suspended in 1 mL PBS and put through a Falcon tube with Cell Strainer Cap (Falcon #08–771-23) to ensure single cell suspension before analysis on a 13-color Becton Dickinson FACSAria III in the Cedars-Sinai Flow Cytometry Core.

FACS analysis

Thresholds distinguishing positive vs. negative cells were established using secondary only negative controls and the percentages of E-cadherin and CDCP1-positive cells determined by double staining with respective antibodies.

Immunocytochemistry/immunofluorescence

E⁻DU145/shControl and shCDCP1 were suspended in HEMA-coated 60 mM tissue culture plates for 3 h. Cells were fixed for 10 min with 3.4% PFA and permeabilized/fixed for 30 min. Cells were spun at $1000 \times g$ for 2 min and re-suspended in 1:1000 primary antibodies in 5% goat serum in PBS for 1 h. Cells were washed with PBS, then incubated with 1:2000 secondary antibodies in 5% goat serum in PBS for 30 min. Cells were washed with PBS, mounted with ProLong Gold Antifade (Life Technologies P36930) and Fisher microscope coverglass (Fisher #12–545-83), allowed to dry overnight, and imaged on a Nikon Eclipse TI inverted fluorescent microscope.

CTCs from patients with CRPC

CTCs were isolated and evaluated via qPCR following the protocol in [35]. Informed consent was obtained from all subjects. Briefly, CTCs were collected from nine patients with castrate-resistant prostate cancer. Patients were required to have histologically confirmed prostate adeno-carcinoma, progressive disease despite "castration levels" of serum testosterone (<50 ng per deciliter [1.73 nmol per liter]) with continued androgen-deprivation therapy, and documented metastases, as confirmed on computed tomography (CT) or bone scanning with technetium-99m-labeled methylene diphosphonate and patients had to have two or more rising serum PSA values obtained 2 or more weeks apart, with the last value being 2.0 ng per milliliter or higher. Blood specimens were collected in Cellsave (Jansen Diagnostics, fixed) or vacutainer tubes (BD Biosciences, live) with EDTA anticoagulant. Mononuclear cells were isolated with a ficoll gradient. EDTA samples were CD45 depleted to improve purity of live cell capture of CTCs. CTCs were isolated with VERSA using an antibody to Epcam conjugated to paramagnetic particles. Downstream mRNA elution sample is integrated on the VERSA. mRNA was reverse transcribed using a high-capacity cDNA reverse transcriptase kit (Life Technologies, USA), according to manufacturer's directions using Bio-Rad C1000 Thermo Cycler (Bio-Rad, USA). The RT reaction (12.5 μL) was then amplified for 10 cycles using TaqMan® PreAmp (Life Technologies, USA) according to manufacturer's directions and diluted 1:5 in 1× TE (10 mM Tris-HCL pH 8, 1 mM EDTA). For TaqMan® assays, 5 μL of diluted cDNA template was mixed with 10 μL iTaq® master mix (Bio-Rad, USA), 1 μL TaqMan® Gene Expression Assay (Life Technologies, USA) and 4 μL nuclease-free (NF) water. Each reaction was amplified for 45 cycles (denatured at 95 °C for 15 s followed by annealing at 60 °C for 1 min) using a CFX Connect® Real-Time PCR System (Bio-Rad, USA).

Computational analysis

Statistical analysis was performed in R Program and data visualization methods as in [3]. We utilized a computationally assembled data set $(n = 1321)$ consists of human prostate cancer transcriptome profiles from 38 distinct cohorts [33]. Differentially expressed genes

were calculated by comparing samples with top and lower 10 percentile CDCP1 expression in the metastatic subset. Genes were ranked by *t*-statistic and GSEA was performed on this rank list. The horizontal lines in the boxplots represent the 1st, 2nd, and 3rd quartiles and whiskers outside the box show the 1.5 interquartile range. The significance of the differences of data illustrated in the boxplots was calculated using the Wilcoxon rank-sum tests. CDCP1 expression in xenografts after IHC staining was scored on a scale of 0–200 by multiplying the percentage of cells that stained (scale 0–100) times the intensity of antibody staining (0, 1, 2), yielding values of expression between 0 and 200.

Mouse studies

Mouse studies were conducted under an IACUC approved protocol from Cedars-Sinai Medical Center. In vivo experiments were conducted in 10 male beige SCID mice randomly assigned to implantation with CDCP1-positive or negative cells according to [74]. Briefly, 1 $\times 10^6$ cells of E⁻DU145/shControl or shCDCP1 were injected into the left and right flank of mice subcutaneously and allowed to grow for 9 weeks before harvest, tumor volume quantification as in [75] and IHC staining according to [76]. Investigators were not blinded to the data.

Preparation of CDCP1-negative cells

Lentiviral silencing of CDCP1 in E⁻DU145 and E⁻PC3 was accomplished with short hairpin sequences generously donated from the Moasser group as described in [11]. Briefly, short hairpin RNA (shRNA) sequences were cloned into pSico-RNeo lentiviral vectors containing a neomycin resistance cassette. For the shCDCP1 #1 construct, the oligonucleotide 5′-TGAATGTTGCTTTCTCGTGGCAGTTCAAGAGACTGCCA-CGAGAAAGCAACATTTTTTTTGGATCC-3′ and for the shCDCP1 #2 construct, the oligonucleotide 5′-TGATAGATGAGCGGTTTGCAATGCTGATTCAAGAGATCAGCATTGCAAACCGCTC ATCTATTTTTTTTGGCGCGCC-3′ was cloned into HpaI and XhoI sites of the pSicoRNeo vector. The shControl construct contains oligonucleotides 5′-TGTCTCGCTTGGGCGAGAGTAAGTTCAAGAGACTTACTCTCGCCCAAGCGAGATT TTTTTGGCGCGCC-3′ and was similarly cloned. The shRNA constructs were transfected into 293T cells and the resulting lentiviral particles were used to infect E⁻DU145 and E⁻PC3 cells. Cells were selected with G418 (400 μg/mL), and CDCP1 knockdown was confirmed by western blotting.

Suspending cells on HEMA-coated plates

1 g Poly-HEMA (Poly (2-hydroxyethyl methacrylate)) (Sigma #P3932) was dissolved in 50 mL 95% ethanol overnight at 37 °C. This 20 mg/mL Poly-HEMA solution was applied to 100 and 60 mM Corning culture dishes at 20 mg/mL and left to dry in the hood for 5 h. A second coat of 20 mg/mL Poly-HEMA was applied and left to dry for 5 h. The culture plates were washed three times with PBS before cells were introduced.

Western blots

E⁻DU145 or E⁻PC3 shControl and shCDCP1 were suspended in HEMA-coated 60 mM tissue culture plates for 6 h. Protein was extracted with radioimmunoprecipitation assay (RIPA) buffer containing 50 mM Tris, 150 mM NaCl, 0.1% sodium dodecyl sulfate (SDS), 0.5% Na deox-ycholate, 1% NP-40 and protease and phosphatase inhibitors. Lysates were kept on ice for 15 min, and then centrifuged $20,000 \times g$ for 10 min at 4°C. Supernatants were mixed with $4\times$ SDS loading dye and denatured at 100 °C for 4 min. Proteins were separated by SDS-polyacrylamide gel electrophoresis, and transferred onto a Hybond-C nitrocellulose membrane (GE Healthcare). Proteins were probed with primary antibody according to manufacturer's instruction and detected with SuperSignal West Pico Chemiluminescent Substrate (ThermoScientific #34080).

Proliferation assay

Five thousand cells of E⁻Du145 or E⁻PC3 shControl and shCDCP1 were seeded into each well of a HEMA-coated 96-well plate format with RPMI media + 10% FBS and $1\times$ Glutamine. The cells were allowed to grow for 24 h. 10 μL of MTT Labeling Reagent (Life Technologies) was added to each well and incubated 4h. 100 μL of MTT Solubility Reagent was added to each well. The plate was read on a spectrophotometer at 570 nm.

Adhesion assay

Five thousand cells of E⁻DU145/shControl and shCDCP1 were seeded into each well of a HEMA-coated 96-well plate format with RPMI media + 10% FBS and $1\times$ Glutamine. The cells were suspended and allowed to grow for 2 and 4h. Unadhered cells were removed and 10 μL of MTT Labeling Reagent (Life Technologies) was added to each well for 4 h. 100 μL of MTT Solubility Reagent was added to each well. The plate was read on a spectrophotometer at 570 nm.

Soft agar colony assay

Twenty thousand E⁻DU145 or E⁻PC3 shControl and shCDCP1 were plated in 60 mM tissue culture plates with 4mL of 1.8% bottom agar (BD Difco Agar) containing RPMI + 10% FBS + $1\times$ Glutamine. The cells were suspended in 0.6% top agar with RPMI + 10% FBS + $1\times$ Glutamine. Six plates were generated for each condition. The cells were allowed to grow for 21 days at which point they were imaged on a Leica microscope. Colony number and diameter were quantified with ImageJ.

Migration assay

Five hundred thousand E⁻DU145 or E⁻PC3 shControl and shCDCP1 were dissociated with EDTA and kept in suspension in HEMA-coated plates for 2 h. Cells were spun down and re-suspended in RPMI media + 1% BSA, then immediately applied to Millipore Millicell 0.8 μM hanging cell culture inserts (#PSET010R5) in 24-well tissue culture plates with RPMI + 10% FBS media in the wells. Cells were allowed to migrate through the filter for 2 h before fixation with 3.4% PFA and staining with Crystal Violet. Non-migratory cells at the top of the hanging insert were removed with a cotton swab. Stained cells that migrated

through the filter were imaged on a Leica microscope and number of cells was quantified with ImageJ.

Co-immunoprecipitation

Co-immunoprecipitations were conducted according to the protocol in [77]. Briefly, the protein concentration of E−Du145 and E−PC3 lysates were determined by Lowry assay (Biorad Dc assay cat: 500, Biorad, UK). Aliquots of cell lysates containing 500 μg protein were transferred to new tubes and the volume adjusted to 400 μL with lysis buffer. 30 μL packed Pierce Protein A/G Plus Agarose Beads (Life Technologies #20423) were combined with 500 μg whole cell lysate on a rocker at 4 °C for 1 h to clear the lysate. 500 μg cleared protein lysate and 5 μg/mL primary antibody were rocked overnight at 4 °C. Control samples had 5 μg isotype-matched control IgG added. 30 μL of fresh packed beads were added to the protein lysate with primary antibody and rocked at 4 °C for 1 h. Samples were centrifuged for 5 min at 10,000 × g. The beads were washed three times with 500 μL immunoprecipitation buffer (20 mM Tris, 100 mM NaCl, 1 mM EDTA, 1% Tween) before applying 25 μL 2× SDS sample buffer (Bio-Rad 161–0737) with 10% β-mercaptoethanol (Sigma-Aldrich M6250) and boiled at 100 °C for 5 min. The samples were centrifuged briefly at room temperature before loading with Prot/Elec tips (Bio-Rad 2239916) on a western blot.

CDK5 kinase activity assay

CDK5 kinase activity was quantified according to [44]. Briefly, E−DU145 cells were lysed with RIPA buffer and protein concentration determined by Lowry assay. Following CDK5 immunoprecipitation on 500 μg protein lysate, a kinase assay was initiated using 10 μM CDK5 substrate peptide and 2 μCi [γ−^{32}P]ATP for 20 min. The supernatant was spotted on phosphocellulose disks, incubated with 10% acetic acid for 30 min, and finally washed with 0.5% H_3PO_4, followed by acetone. ^{32}P incorporation on CDK5 substrate peptide was measured using a scintillation counter.

Double transfection

siRNA was purchased from Dharmacon (100 Results Way Marlborough, MA 01752). 250 μM Dharmacon SMART-pool: ON-TARGETplus PRKCD siRNA (L-003524–00-0005) in NF water was electroporated into 5 × 10^6 S-DU145 shControl and shCDCP1 according to manufacturer's optimized protocol for this cell line (Life Technologies, #MPK5000). Briefly, E−DU145 cells were electroporated with two pulses of 1260 V. Cell lysate was collected and assessed for PKCδ and CDCP1 double knockdown at 48 and 72 h timepoints via western blot.

PKCδ constructs

PKCδ constructs were purchased from Addgene (75 Sidney Street, Suite 550A Cambridge, MA 02139). PKCδ-C2 domain (Addgene #16388) and wild-type PKCδ (Addgene #16386) were cloned into lentiviral vector pLenti-C-mGFP from OriGene (9620 Medical Center Dr., Suite 200, Rockville, MD 20850) (PS100071) via EcoRI digestion and ligation and

transfected via electroporation using a Neon transfection system. 48 h later, positive cells were selected by FACS sorting GFP + population.

PKCδ DN was a gift from Bernard Weinstein (Addgene plasmid # 16389). PKCδ DN contains a K376R mutation. PKCδ DN and wild-type PKCδ (Plasmid #16386) were cloned into OriGene pLenti-C-mGFP (PS100071) and transfected via electroporation into E⁻DU145 shCDCP1. After 48 h, cells positive for PKCδ DN were selected via FACS sorting the GFP + population.

CDK5 and CDK5R1/p35 constructs

CDK5 mutant design was conducted as described in [78]. CDK5 mutants were generated at GENEWIZ (3235 Grande Vista Drive Newbury Park, CA 91320). CDK5-Myc-DDK (RC200342) and pLenti-C-Myc-DDK-IRES-Puro vector (PS100069) were purchased from Origene and sent to GENEWIZ. GENEWIZ performed synthesis of CDK5-T77A mutant (ACT to GCT) and CDK5-T77D mutant (ACT to GAT) by adding 5′(BamHI) and 3′(NheI) sequences, and using site-specific mutagenesis at position 271 to change ACT to GCT (Mutant #1) and to change ACT to GAT (Mutant #2). GENEWIZ performed sequence verification and custom cloning into pLenti-C-Myc-DDK-IRES-Puro (Kanamycin) via 5′ BamHI and 3′NheI. The CDK5 constructs were transfected via electroporation into E⁻DU145 shControl and shCDCP1. Positive cells were selected via treatment with 5 μg/mL Puromycin. Co-immunoprecipitations of the mutants with MYC-tag antibody were performed as described above.

CDK5R1/p35 constructs

CDK5R1/p35 mutants were generated at GENEWIZ (3235 Grande Vista Drive Newbury Park, CA 91320). GENEWIZ obtained a CDK5R1/p35 clone and sequenced the clone for verification. GENEWIZ performed synthesis of Mutant #1 (Y231 to F) and Mutant #2 (Y234 to F) by using site-specific mutagenesis to change 379 TAC to TTC (Mutant #1) and to change TAC to TTC (Mutant #2). GENEWIZ performed sequence verification and custom cloning into pLenti-C-Myc-DDK-IRES-Puro (Kanamycin) via 5′BamHI and 3′ NheI. The CDK5R1/p35 constructs were transfected by themselves or together with PKC mutants via electroporation into E⁻DU145 shCDCP1. Positive cells were selected via treatment with 5 μg/mL puromycin. Co-immunoprecipitations of the mutants with MYC-tag antibody were performed as described above.

Supplementary Material

Refer to Web version on PubMed Central for supplementary material.

Acknowledgements

References

1. Wortmann A, He Y, Deryugina EI, Quigley JP, Hooper JD. The cell surface glycoprotein CDCP1 in cancer—insights, opportunities, and challenges. IUBMB Life. 2009;61:723–30. [PubMed: 19514048]

2. Siva AC, Kirkland RE, Lin B, Maruyama T, McWhirter J, Yantiri-Wernimont F, et al. Selection of anti-cancer antibodies from combinatorial libraries by whole-cell panning and stringent subtraction with human blood cells. J Immunol Methods. 2008;330:109–19. [PubMed: 18096183]

3. Siva AC, Wild MA, Kirkland RE, Nolan MJ, Lin B, Maruyama T, et al. Targeting CUB domain-containing protein 1 with a monoclonal antibody inhibits metastasis in a prostate cancer model. Cancer Res. 2008;68:3759–66. [PubMed: 18483259]

4. Deryugina EI, Conn EM, Wortmann A, Partridge JJ, Kupriyanova TA, Ardi VC, et al. Functional role of cell surface CUB domain-containing protein 1 in tumor cell dissemination. Mol Cancer Res. 2009;7:1197–211. [PubMed: 19671673]

5. Fukuchi K, Steiniger SC, Deryugina E, Liu Y, Lowery CA, Gloeckner C, et al. Inhibition of tumor metastasis: functional immune modulation of the CUB domain containing protein 1. Mol Pharm. 2010;7:245–53. [PubMed: 19916495]

6. Zarif JC, Lamb LE, Schulz VV, Nollet EA, Miranti CK. Androgen receptor non-nuclear regulation of prostate cancer cell invasion mediated by Src and matriptase. Oncotarget. 2015;6:6862–76. [PubMed: 25730905]

7. Casar B, He Y, Iconomou M, Hooper JD, Quigley JP, Deryugina EI. Blocking of CDCP1 cleavage in vivo prevents Akt-dependent survival and inhibits metastatic colonization through PARP1-mediated apoptosis of cancer cells. Oncogene. 2012;31:3924–38. [PubMed: 22179830]

8. Yang L, Dutta SM, Troyer DA, Lin JB, Lance RA, Nyalwidhe JO, et al. Dysregulated expression of cell surface glycoprotein CDCP1 in prostate cancer. Oncotarget. 2015;6:43743–58. [PubMed: 26497208]

9. Sandvig K, Llorente A. Proteomic analysis of microvesicles released by the human prostate cancer cell line PC-3. Mol Cell Proteom. 2012;11:M111.012914.

10. Minciacchi VR, Zijlstra A, Rubin MA, Di Vizio D. Extracellular vesicles for liquid biopsy in prostate cancer: where are we and where are we headed? Prostate Cancer Prostatic Dis. 2017;20:251–8. [PubMed: 28374743]

11. Spassov DS, Wong CH, Wong SY, Reiter JF, Moasser MM. Trask loss enhances tumorigenic growth by liberating integrin signaling and growth factor receptor cross-talk in unanchored cells. Cancer Res. 2013;73:1168–79. [PubMed: 23243018]

12. Dong Y, He Y, de Boer L, Stack MS, Lumley JW, Clements JA, et al. The cell surface glycoprotein CUB domain-containing protein 1 (CDCP1) contributes to epidermal growth factor receptor-mediated cell migration. J Biol Chem. 2012;287:9792–803. [PubMed: 22315226]

13. Spassov DS, Wong CH, Moasser MM. Trask phosphorylation defines the reverse mode of a phosphotyrosine signaling switch that underlies cell anchorage state. Cell Cycle. 2011;10:1225–32. [PubMed: 21490433]

14. DeVries-Seimon TA, Ohm AM, Humphries MJ, Reyland ME. Induction of apoptosis is driven by nuclear retention of protein kinase C delta. J Biol Chem. 2007;282:22307–14. [PubMed: 17562707]

15. Spassov DS, Baehner FL, Wong CH, McDonough S, Moasser MM. The transmembrane Src substrate Trask is an epithelial protein that signals during anchorage deprivation. Am J Pathol. 2009;174:1756–65. [PubMed: 19349359]

16. Wright HJ, Arulmoli J, Motazedi M, Nelson LJ, Heinemann FS, Flanagan LA, et al. CDCP1 cleavage is necessary for homodimerization-induced migration of triple-negative breast cancer. Oncogene. 2016;35:4762–72. [PubMed: 26876198]

17. Alvares SM, Dunn CA, Brown TA, Wayner EE, Carter WG. The role of membrane microdomains in transmembrane signaling through the epithelial glycoprotein Gp140/CDCP1. Biochim Biophys Acta. 2008;1780:486–96. [PubMed: 18269919]

18. Casar B, Rimann I, Kato H, Shattil SJ, Quigley JP, Deryugina EI. In vivo cleaved CDCP1 promotes early tumor dissemination via complexing with activated beta1 integrin and induction of FAK/PI3K/Akt motility signaling. Oncogene. 2014;33:255–68. [PubMed: 23208492]

19. Takagi J, Petre BM, Walz T, Springer TA. Global conformational rearrangements in integrin extracellular domains in outside-in and inside-out signaling. Cell. 2002;110:599–611. [PubMed: 12230977]

20. Moser M, Legate KR, Zent R, Fässler R. The tail of integrins, talin, and kindlins. Science. 2009;324:895–9. [PubMed: 19443776]

21. Shattil SJ, Kim C, Ginsberg MH. The final steps of integrin activation: the end game. Nat Rev Mol Cell Biol. 2010;11:288–300. [PubMed: 20308986]

22. Schwartz MA, Schaller MD, Ginsberg MH. Integrins: emerging paradigms of signal transduction. Annu Rev Cell Dev Biol. 1995;11:549–99. [PubMed: 8689569]

23. Provasi D, Negri A, Coller BS, Filizola M. Talin-driven inside-out activation mechanism of platelet αIIbβ3 integrin probed by multimicrosecond, all-atom molecular dynamics simulations. Proteins. 2014;82:3231–40. [PubMed: 24677266]

24. Ginsberg MH. Integrin activation. BMB Rep. 2014;47:655–9. [PubMed: 25388208]

25. Jin JK, Tien PC, Cheng CJ, Song JH, Huang C, Lin SH, et al. Talin1 phosphorylation activates β1 integrins: a novel mechanism to promote prostate cancer bone metastasis. Oncogene. 2015;34:1811–21. [PubMed: 24793790]

26. Hsu FN, Chen MC, Chiang MC, Lin E, Lee YT, Huang PH, et al. Regulation of androgen receptor and prostate cancer growth by cyclin-dependent kinase 5. J Biol Chem. 2011;286:33141–9. [PubMed: 21799006]

27. Strock CJ, Park JI, Nakakura EK, Bova GS, Isaacs JT, Ball DW, et al. Cyclin-dependent kinase 5 activity controls cell motility and metastatic potential of prostate cancer cells. Cancer Res. 2006;66:7509–15. [PubMed: 16885348]

28. Sato K, Zhu YS, Saito T, Yotsumoto K, Asada A, Hasegawa M, et al. Regulation of membrane association and kinase activity of Cdk5-p35 by phosphorylation of p35. J Neurosci Res. 2007;85:3071–8. [PubMed: 17671990]

29. Gao C, Negash S, Guo HT, Ledee D, Wang HS, Zelenka P. CDK5 regulates cell adhesion and migration in corneal epithelial cells. Mol Cancer Res. 2002;1:12–24. [PubMed: 12496365]

30. Nakano N, Nakao A, Ishidoh K, Tsuboi R, Kominami E, Okumura K, et al. CDK5 regulates cell-cell and cell-matrix adhesion in human keratinocytes. Br J Dermatol. 2005;153:37–45.

31. Bosutti A, Qi J, Pennucci R, Bolton D, Matou S, Ali K, et al. Targeting p35/Cdk5 signalling via CIP-peptide promotes angio-genesis in hypoxia. PLoS ONE. 2013;8:e75538.

32. Tsai LH, Delalle I, Caviness VS, Chae T, Harlow E. p35 is a neural-specific regulatory subunit of cyclin-dependent kinase 5. Nature. 1994;371:419–23. [PubMed: 8090221]

33. You S, Knudsen BS, Erho N, Alshalalfa M, Takhar M, Al-Deen Ashab H, et al. Integrated classification of prostate cancer reveals a novel luminal subtype with poor outcome. Cancer Res. 2016;76:4948–58. [PubMed: 27302169]

34. Das L, Anderson TA, Gard JM, Sroka IC, Strautman SR, Nagle RB, et al. Characterization of laminin binding integrin internalization in prostate cancer cells. J Cell Biochem. 2017;118:1038–49. [PubMed: 27509031]

35. Sperger JM, Strotman LN, Welsh A, Casavant BP, Chalmers Z, Horn S. et al. Integrated analysis of multiple biomarkers from circulating tumor cells enabled by exclusion-based analyte isolation. Clin Cancer Res. 2016;23:746–756. [PubMed: 27401243]

36. Putzke AP, Ventura AP, Bailey AM, Akture C, Opoku-Ansah J, Celikta M, et al. Metastatic progression of prostate cancer and E- cadherin regulation by zeb1 and SRC family kinases. Am J Pathol. 2011;179:400–10. [PubMed: 21703419]

37. Schehr JL, Schultz ZD, Warrick JW, Guckenberger DJ, Pezzi HM, Sperger JM, et al. High specificity in circulating tumor cell identification is required for accurate evaluation of programmed death-ligand 1. PLoS ONE. 2016;11:e0159397.

38. Kimura H, Morii E, Ikeda JI, Ezoe S, Xu JX, Nakamichi N, et al. Role of DNA methylation for expression of novel stem cell marker CDCP1 in hematopoietic cells. Leukemia. 2006;20:1551–6. [PubMed: 16926850]

39. Tun HW, Marlow LA, von Roemeling CA, Cooper SJ, Kreinest P, Wu K, et al. Pathway signature and cellular differentiation in clear cell renal cell carcinoma. PLoS ONE. 2010;5:e10696.

40. Cantu E, Lederer DJ, Meyer K, Milewski K, Suzuki Y, Shah RJ, et al. Gene set enrichment analysis identifies key innate immune pathways in primary graft dysfunction after lung transplantation. Am J Transplant. 2013;13:1898–904. [PubMed: 23710539]

41. Spassov DS, Wong CH, Sergina N, Ahuja D, Fried M, Sheppard D, et al. Phosphorylation of Trask by Src kinases inhibits integrin clustering and functions in exclusion with focal adhesion signaling. Mol Cell Biol. 2011;31:766–82. [PubMed: 21189288]

42. Calderwood DA, Campbell ID, Critchley DR. Talins and kindlins: partners in integrin-mediated adhesion. Nat Rev Mol Cell Biol. 2013;14:503–17. [PubMed: 23860236]

43. Hisanaga S, Saito T. The regulation of cyclin-dependent kinase 5 activity through the metabolism of p35 or p39 Cdk5 activator. Neurosignals. 2003;12:221–9. [PubMed: 14673209]

44. Chang KH, Multani PS, Sun KH, Vincent F, de Pablo Y, Ghosh S, et al. Nuclear envelope dispersion triggered by deregulated Cdk5 precedes neuronal death. Mol Biol Cell. 2011;22:1452–62. [PubMed: 21389115]

45. Wortmann A, He Y, Christensen ME, Linn M, Lumley JW, Pollock PM, et al. Cellular settings mediating Src substrate switching between focal adhesion kinase tyrosine 861 and CUB-domain-containing protein 1 (CDCP1) tyrosine 734. J Biol Chem. 2011;286:42303–15. [PubMed: 21994943]

46. Stahelin RV, Kong KF, Raha S, Tian W, Melowic HR, Ward KE, et al. Protein kinase C0 C2 domain is a phosphotyrosine binding module that plays a key role in its activation. J Biol Chem. 2012;287:30518–28. [PubMed: 22787157]

47. Benes CH, Wu N, Elia AE, Dharia T, Cantley LC, Soltoff SP. The C2 domain of PKCdelta is a phosphotyrosine binding domain. Cell. 2005;121:271–80. [PubMed: 15851033]

48. Li W, Yu JC, Shin DY, Pierce JH. Characterization of a protein kinase C-delta (PKC-delta) ATP binding mutant. An inactive enzyme that competitively inhibits wild type PKC-delta enzymatic activity. J Biol Chem. 1995;270:8311–8. [PubMed: 7713939]

49. Uekita T, Jia L, Narisawa-Saito M, Yokota J, Kiyono T, Sakai R. CUB domain-containing protein 1 is a novel regulator of anoikis resistance in lung adenocarcinoma. Mol Cell Biol. 2007;27:7649–60. [PubMed: 17785447]

50. Uekita T, Tanaka M, Takigahira M, Miyazawa Y, Nakanishi Y, Kanai Y, et al. CUB-domain-containing protein 1 regulates peritoneal dissemination of gastric scirrhous carcinoma. Am J Pathol. 2008;172:1729–39. [PubMed: 18467693]

51. Sachdev S, Bu Y, Gelman IH. Paxillin-Y118 phosphorylation contributes to the control of Src-induced anchorage-independent growth by FAK and adhesion. BMC Cancer. 2009;9:12. [PubMed: 19138410]

52. Razorenova OV, Finger EC, Colavitti R, Chernikova SB, Boiko AD, Chan CK, et al. VHL loss in renal cell carcinoma leads to up-regulation of CUB domain-containing protein 1 to stimulate PKC {delta}-driven migration. Proc Natl Acad Sci USA. 2011;108:1931–6. [PubMed: 21233420]

53. Benes CH, Poulogiannis G, Cantley LC, Soltoff SP. The SRC-associated protein CUB domain-containing protein-1 regulates adhesion and motility. Oncogene. 2012;31:653–63. [PubMed: 21725358]

54. Liu H, Ong SE, Badu-Nkansah K, Schindler J, White FM, Hynes RO. CUB-domain-containing protein 1 (CDCP1) activates Src to promote melanoma metastasis. Proc Natl Acad Sci USA. 2011;108:1379–84. [PubMed: 21220330]

55. Liu Y, Belkina NV, Graham C, Shaw S. Independence of protein kinase C-delta activity from activation loop phosphorylation: structural basis and altered functions in cells. J Biol Chem. 2006;281:12102–11. [PubMed: 16505477]

56. O'Hare MJ, Kushwaha N, Zhang Y, Aleyasin H, Callaghan SM, Slack RS, et al. Differential roles of nuclear and cytoplasmic cyclin-dependent kinase 5 in apoptotic and excitotoxic neuronal death. J Neurosci. 2005;25:8954–66. [PubMed: 16192386]

57. Uekita T, Sakai R. Roles of CUB domain-containing protein 1 signaling in cancer invasion and metastasis. Cancer Sci. 2011;102:1943–8. [PubMed: 21812858]

58. Hofmann J Protein kinase C isozymes as potential targets for anticancer therapy. Curr Cancer Drug Targets. 2004;4:125–46. [PubMed: 15032665]

59. Kawauchi T Cell adhesion and its endocytic regulation in cell migration during neural development and cancer metastasis. Int J Mol Sci. 2012;13:4564–90. [PubMed: 22605996]

60. Ganguly KK, Pal S, Moulik S, Chatterjee A. Integrins and metastasis. Cell Adh Migr. 2013;7:251–61. [PubMed: 23563505]

61. Spassov DS, Wong CH, Harris G, McDonough S, Phojanakong P, Wang D, et al. A tumor-suppressing function in the epithelial adhesion protein Trask. Oncogene. 2012;31:419–31. [PubMed: 21706059]

62. Ohlsson L, Israelsson A, Öberg Å, Palmqvist R, Stenlund H, Hammarström ML, et al. Lymph node CEA and MUC2 mRNA as useful predictors of outcome in colorectal cancer. Int J Cancer. 2012;130:1833–43. [PubMed: 21618511]

63. Mamat S, Ikeda J, Enomoto T, Ueda Y, Rahadiani N, Tian T, et al. Prognostic significance of CUB domain containing protein expression in endometrioid adenocarcinoma. Oncol Rep. 2010;23:1221–7. [PubMed: 20372833]

64. Sawada G, Takahashi Y, Niida A, Shimamura T, Kurashige J, Matsumura T, et al. Loss of CDCP1 expression promotes invasiveness and poor prognosis in esophageal squamous cell carcinoma. Ann Surg Oncol. 2014;21:S640–7. [PubMed: 24849519]

65. Kato H, Liao Z, Mitsios JV, Wang HY, Deryugina EI, Varner JA, et al. The primacy of ß1 integrin activation in the metastatic cascade. PLoS ONE. 2012;7:e46576.

66. Parvani JG, Galliher-Beckley AJ, Schiemann BJ, Schiemann WP. Targeted inactivation of ß1 integrin induces ß3 integrin switching, which drives breast cancer metastasis by TGF-ß. Mol Biol Cell. 2013;24:3449–59. [PubMed: 24006485]

67. Twardowski PW, Beumer JH, Chen CS, Kraft AS, Chatta GS, Mitsuhashi M, et al. A phase II trial of dasatinib in patients with metastatic castration-resistant prostate cancer treated previously with chemotherapy. Anticancer Drugs. 2013;24:743–53. [PubMed: 23652277]

68. Dickreuter E, Eke I, Krause M, Borgmann K, van Vugt MA, Cordes N. Targeting of ß1 integrins impairs DNA repair for radiosensitization of head and neck cancer cells. Oncogene. 2016;35:1353–62. [PubMed: 26073085]

69. Hoffmann A, Lannert H, Brischwein K, Pipp FC, Reindl J, Groll K, et al. inventors; Merck Patent GmbH, Assignee. Anti-alpha-V integrin antibody for the treatment of prostate cancer. 2017; US Patent 9555110, International PCT/EP2012/000548.

70. Antal CE, Hudson AM, Kang E, Zanca C, Wirth C, Stephenson NL, et al. Cancer-associated protein kinase C mutations reveal kinase's role as tumor suppressor. Cell. 2015;160:489–502. [PubMed: 25619690]

71. Blake RA, Garcia-Paramio P, Parker PJ, Courtneidge SA. Src promotes PKCdelta degradation. Cell Growth Differ. 1999;10:231–41. [PubMed: 10319993]

72. Glaser KB, Sung A, Bauer J, Weichman BM. Regulation of eicosanoid biosynthesis in the macrophage. Involvement of protein tyrosine phosphorylation and modulation by selective protein tyrosine kinase inhibitors. Biochem Pharmacol. 1993;45:711–21. [PubMed: 8442770]

73. Yang J, Zheng Z, Yan X, Li X, Liu Z, Ma Z. Integration of autophagy and anoikis resistance in solid tumors. Anat Rec. 2013;296:1501–8.

74. Li X, Wu JB, Li Q, Shigemura K, Chung LW, Huang WC. SREBP-2 promotes stem cell-like properties and metastasis by transcriptional activation of c-Myc in prostate cancer. Oncotarget. 2016;7:12869–84. [PubMed: 26883200]

75. Schiewer MJ, Goodwin JF, Han S, Brenner JC, Augello MA, Dean JL, et al. Dual roles of PARP-1 promote cancer growth and progression. Cancer Discov. 2012;2:1134–49. [PubMed: 22993403]

76. Knudsen BS, Zhao P, Resau J, Cottingham S, Gherardi E, Xu E, et al. A novel multipurpose monoclonal antibody for evaluating human c-Met expression in preclinical and clinical settings. Appl Immunohistochem Mol Morphol. 2009;17:57–67. [PubMed: 18815565]

77. Orchard-Webb DJ, Lee TC, Cook GP, Blair GE. CUB domain containing protein 1 (CDCP1) modulates adhesion and motility in colon cancer cells. BMC Cancer. 2014;14:754. [PubMed: 25301083]

78. Rai AC, Singh I, Singh M, Shah K. Expression of ZAT12 transcripts in transgenic tomato under various abiotic stresses and modeling of ZAT12 protein in silico. Biometals. 2014;27:1231–47. [PubMed: 25187181]
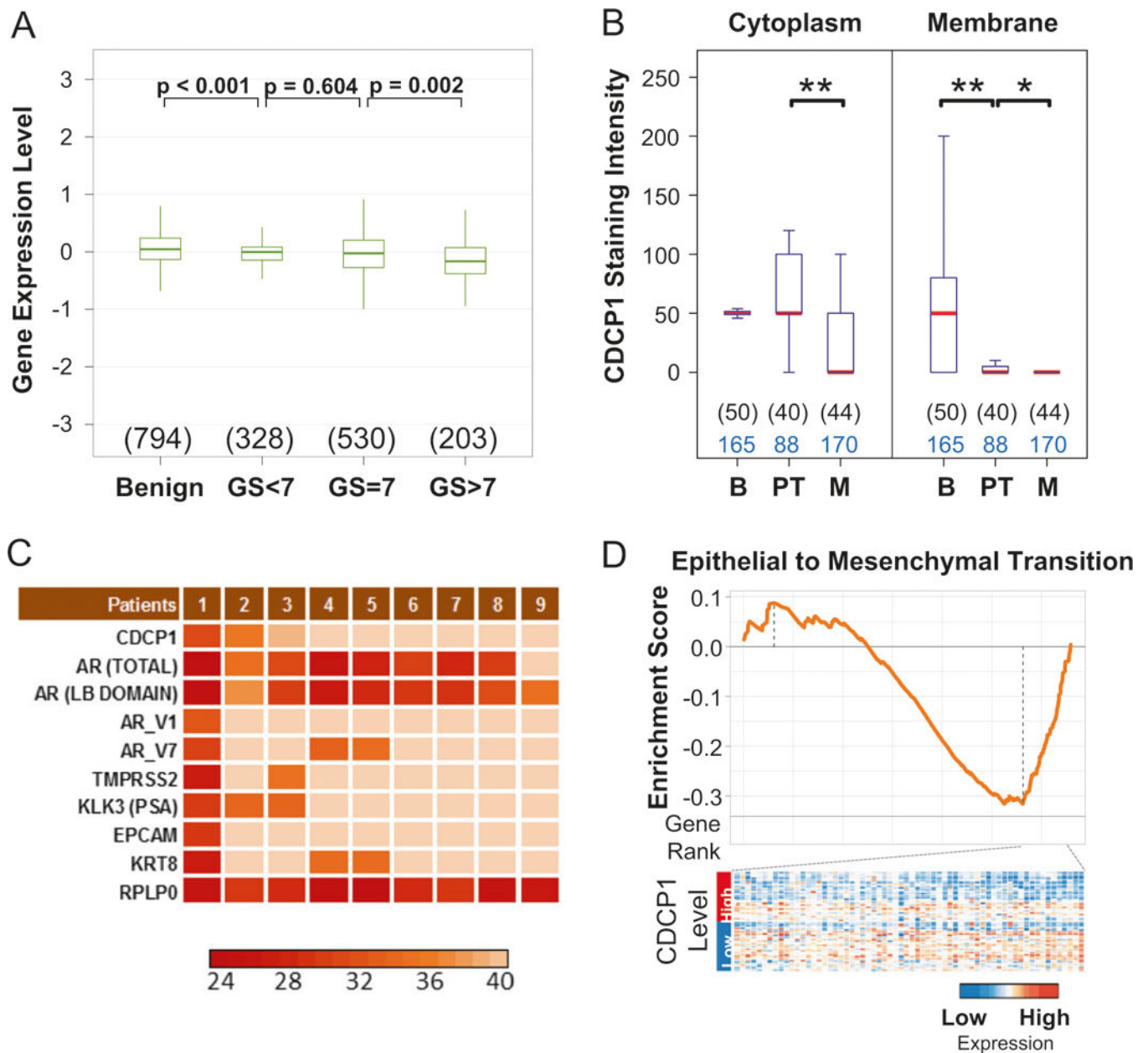
Fig. 1.
CDCP1 expression decreases in advanced prostate cancer. **a** CDCP1 gene expression in an integrated human prostate cancer cohort ($n = 1321$) of transcriptome profiles (PCTA) [33]. The *x*-axis denotes samples of benign, Gleason Sum < 7, Gleason Sum = 7, Gleason Sum > 7 prostate cancer. Numbers in parenthesis indicate samples in each group. Wilcoxon rank-sum tests *p*-values are shown above the box-plots. **b** CDCP1 protein expression levels in benign (B), primary tumor (PT), and metastases (M) from patients measure after staining of a TMA described in [36] by immunohistochemistry. The staining intensity of CDCP1 was separately scored in the membrane and cytoplasm using a categorical scoring scheme. Numbers in parenthesis indicate samples in each group, with each sample represented in duplicate or triplicate on the TMA. **c** Expression of CDCP1 mRNA in circulating tumor

cells. mRNA expression levels of 10 genes were determined in CTCs from each of 9 patients with castrate-resistant prostate cancer (CRPC). A heatmap of qPCR cycle numbers of the Androgen Receptor (AR), AR variant 1 (V1), AR variant 7 (V7), keratin 8 (KRT8), Transmembrane Protease, Serine 2 (TMPRSS2), Kallikrein-3 (KLK3), 60S acidic ribosomal protein P0 (RPLP0). Patients 1–3 had detectable CDCP1 gene expression. **d** GSEA enrichment plot of EMT signature genes associated with loss of CDCP1 expression in CRPC from the PCTA ($n = 260$). The heat map displays the expression of leading edge genes from GSEA analysis in samples with high vs. low CDCP1 expression. *P<0.05 and **P< 0.01
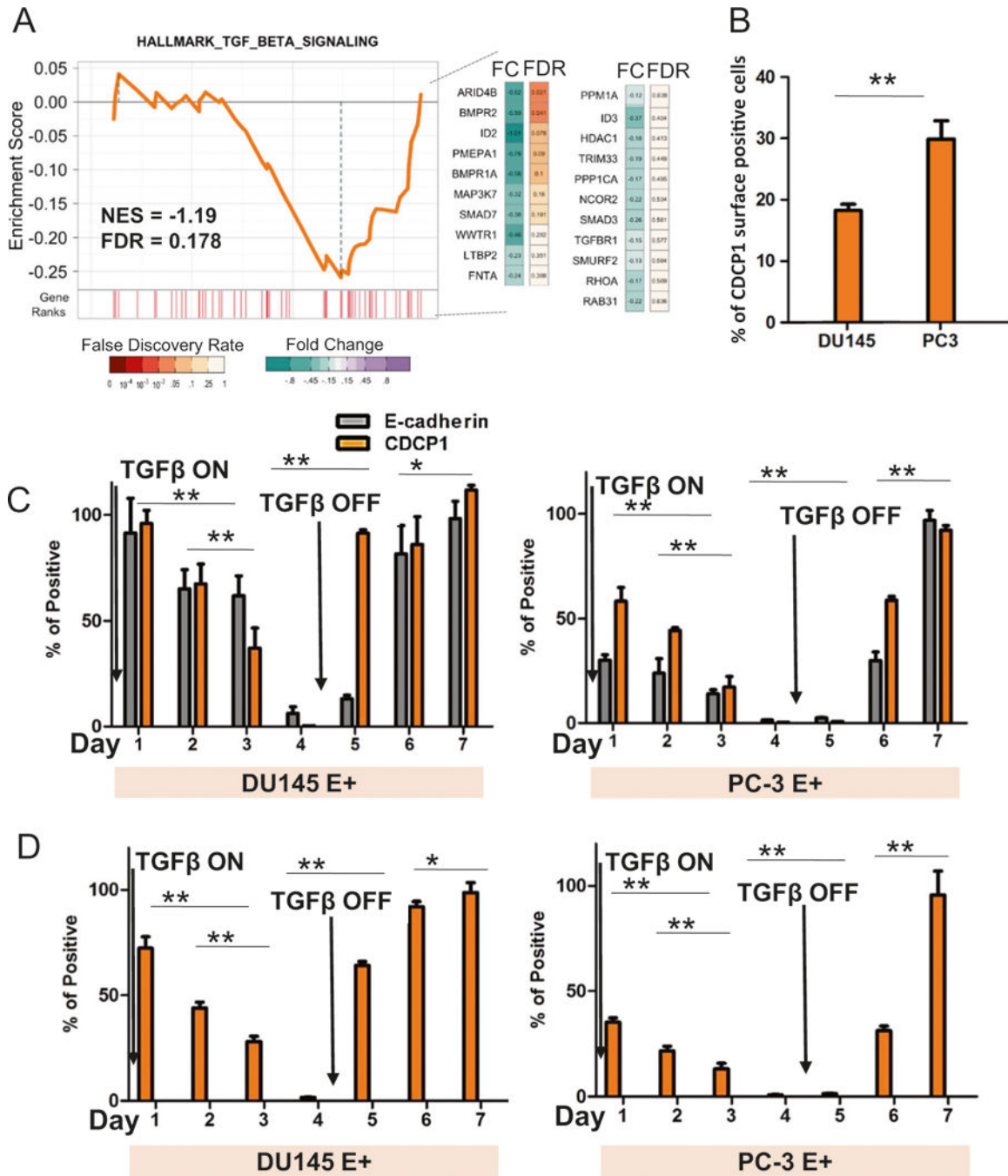
Fig. 2.

TGFβ1 induces reversible loss of CDCP1 expression. **a** GSEA analysis of the hallmark TGFβ1 signature from 260 cases of metastatic prostate cancer [33]. Gene in the leading edge are indicated beside the graph. **b** FACS analysis of CDCP1 protein in E-cadherin-positive DU145 and PC3 prostate cancer cell lines. All cells are E-cadherin positive. The percentage of cells that are positive for CDCP1 is indicated on the *y*-axis. **c, d** Changes in CDCP1 and E-cadherin surface expression (**c**) or mRNA expression (**d**) in E+ DU145 and E+ PC3 cells

after treatment with TGFβ1. TGFβ1 was removed from the culture medium on day 5 and cells grown for an additional 3 days. *$P < 0.05$ and **$P < 0.01$
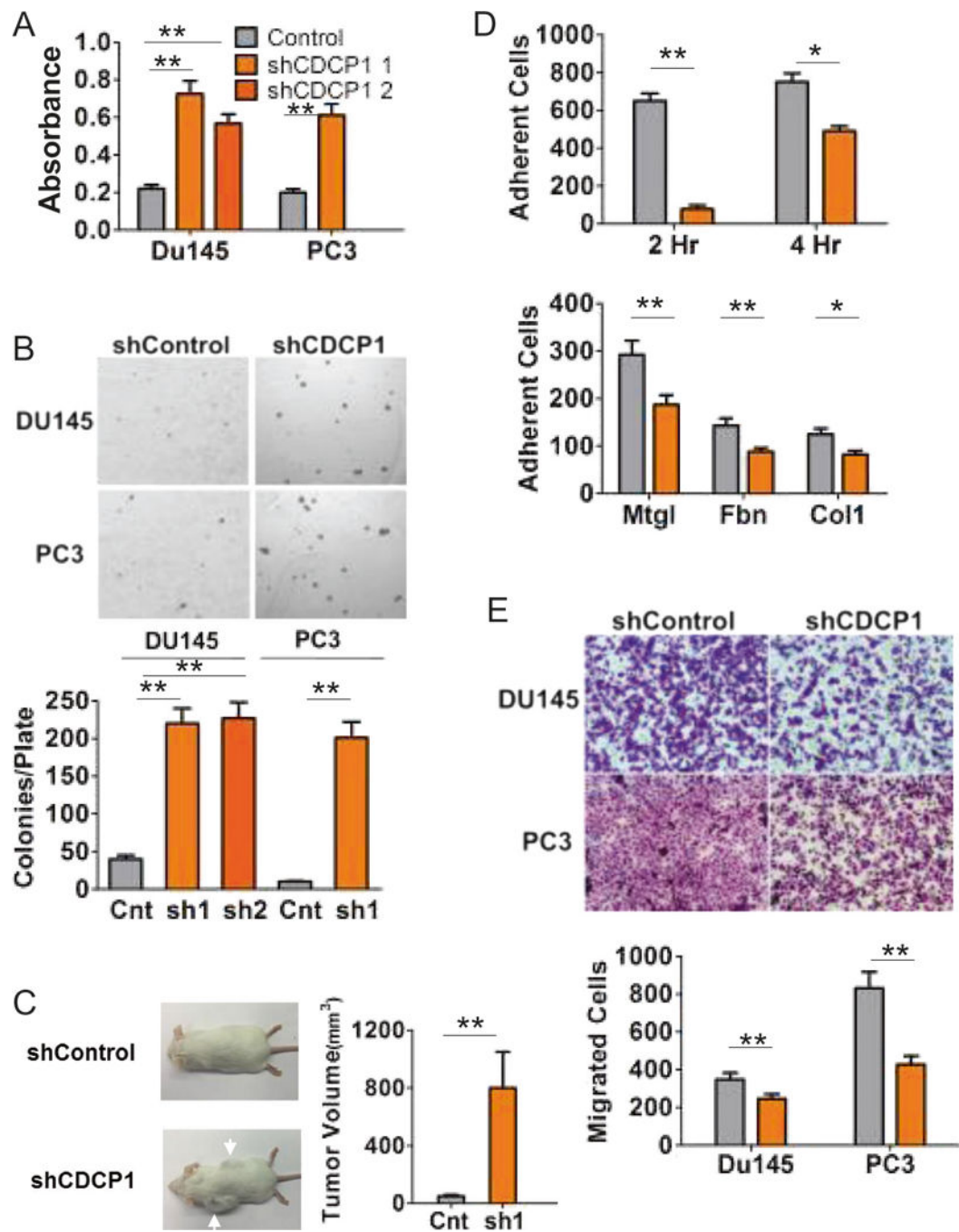
Fig. 3.

CDCP1 loss changes cell behavior. **a** MTT assay of DU145 and PC3 CDCP1 knockdown (shCDCP1) or control hairpin (Control) cells suspended in a HEMA-coated 96-well plate for 24 h. **b** Soft agar colony formation assay of DU145 and PC3 shControl and CDCP1 knockdown (shCDCP1). Colonies were quantified using ImageJ. **c** Xenograft mouse model. 1×10^6 DU145+/−CDCP1 were injected subcutaneously in 9-week-old male beige SCID mice. Tumors were harvested after 9 weeks and the volumes shown in the bar graph. **d** Adhesion assay of DU145 shControl (gray bars) and CDCP1 knockdown shCDCP1 (orange

bars). Cells were adhered for 2 or 4 h to surfaces coated with Matrigel (Mtgl), Fibronectin (Fbn), or Collagen I (Col1). Adherent cell numbers per 20× field, averaged from eight measurements, are plotted on the *y*-axis. **e** Serum (10%)-induced migration assay of DU145 and PC3 through a 0.8 μM Transwell membrane. Migrated cells were stained using crystal violet and quantified with ImageJ. $*P < 0.05$ and $**P < 0.01$
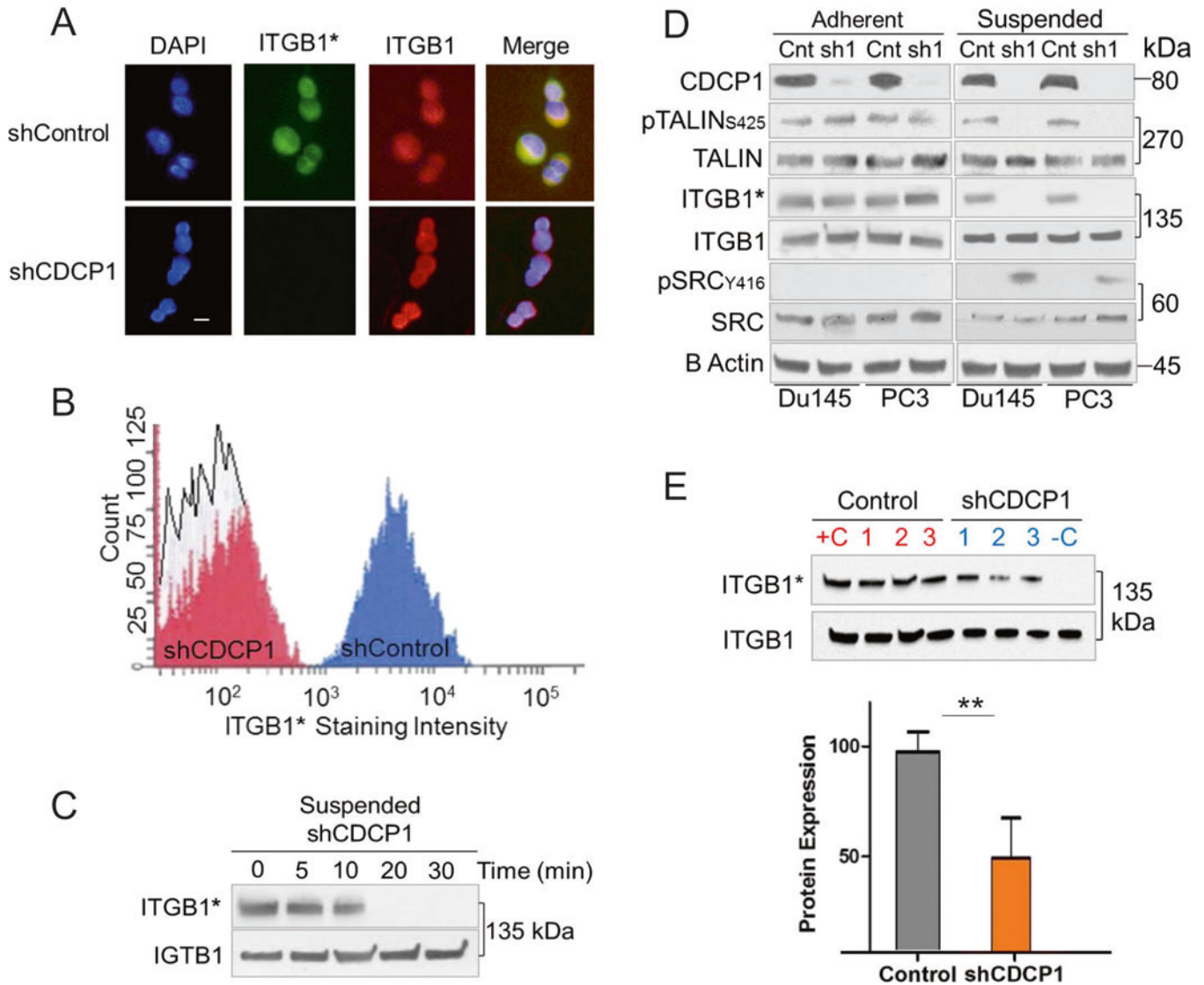
Fig. 4.
CDCP1 silencing inhibits inside-out activation of ITGB1/β1-integrin and activates c-SRC in suspended cells. **a** Immunofluorescent staining of CDCP1-positive (shControl) and negative (shCDCP1) DU145 cells on coverslips. The HUTS-4 antibody was used to determine the activation state of ITGB1/β1-integrin (green: active ITGB1*), total ITGB1/β1-integrin (red), and nuclei (blue). White bar = 10 μM. **b** FACS analysis with HUTS-4 antibody. The staining intensity with HUTS-4 is plotted on the *x*-axis. The *y*-axis reveals the number of cells. **c** Time course of ITGB1/β1-integrin inactivation Active ITGB1/β1-integrin (ITGB1*) and total ITGB1/β1-integrin (ITGB1) were measured after suspending DU145 CDCP1 knockdown cells for the times indicated. **d** Activation of ITGB1/β1-integrin in adherent and suspended (3 h) DU145 and PC3 cells. Cells were analyzed after CDCP1 (sh1) or scrambled control (Cnt) knockdown. **e** Active ITGB1/β1-integrin (ITGB1*) and total ITGB1/β1-integrin (ITGB1) in protein lysates from three control and CDCP1-silenced xenografts [1–

3]. Quantification normalized to total ITGB1/β1-integrin on y-axis. $*P < 0.05$ and $**P < 0.01$
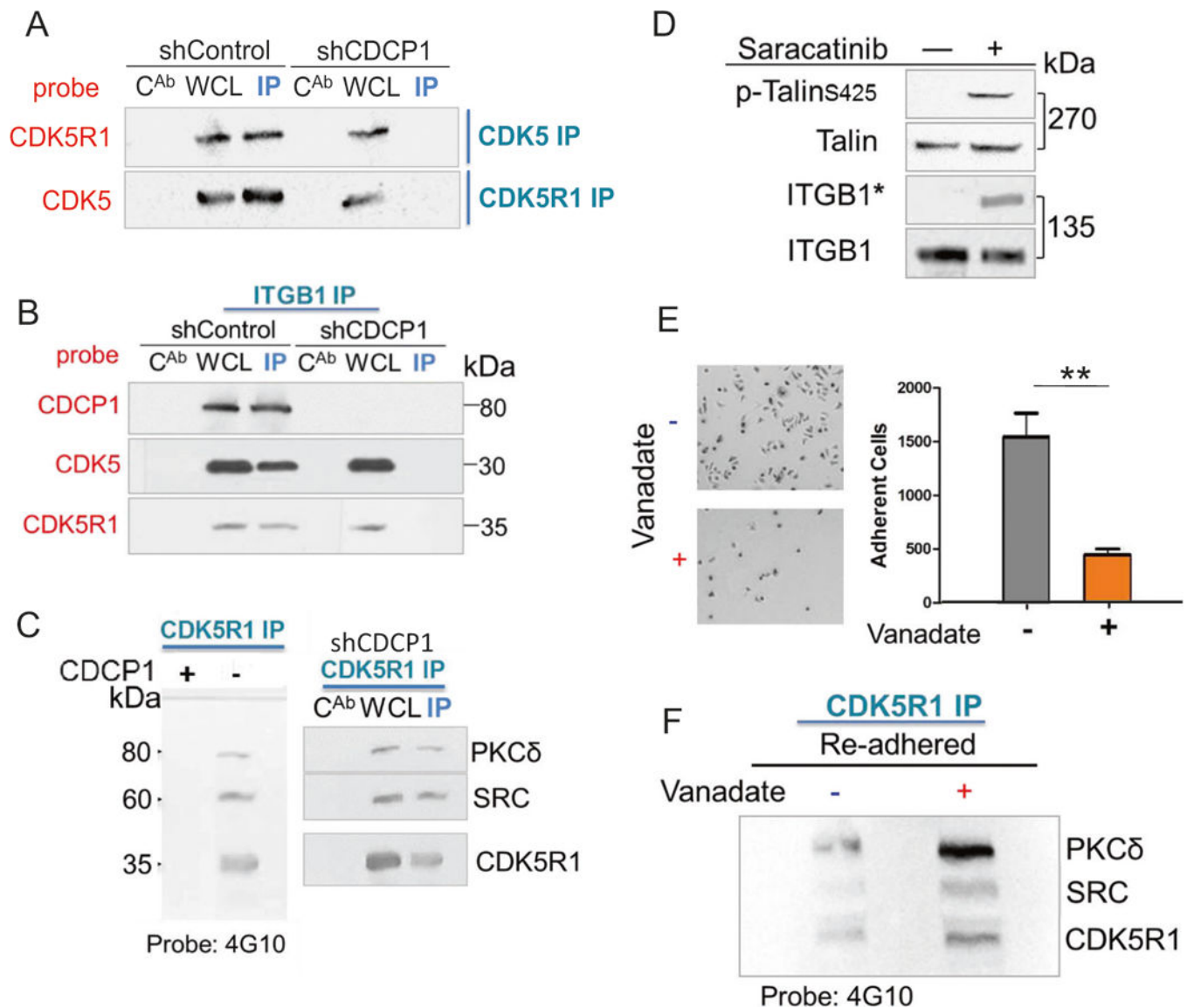
Fig. 5.
De novo phosphorylation of CDCK5R1 after silencing of CDCP1. **a** Loss of CDK5R1-CDK5 complex formation in suspended CDCPl-silenced cells. Reciprocal immunoprecipitations of CDK5 or CDK5R1. WCL whole cell lysate, C^{AB} IgG control, IP immunopre-cipitate. **b** ITGB1-CDK5 complex formation. Western blot of ITGB1/β1-integrin immunoprecipitation (ITGB1 IP) from DU145 cells with and without silencing of CDCP1 and probed for CDCP1, CDK5, and CDK5R1. **c** CDK5R1 immunoprecipitation of suspended DU145/ shCDCPl. CDK5R1 complexes from DU145/shControl (Cnt) or shCDCPl(shl) were probed with the 4G10 antibody. Western blot membranes were re-probed with antibodies reactive to PKCδ, SRC and CDK5R1. **d** Regulation of ITGB1/β1-integrin inside-out activity by c-SRC. DU145/shCDCP1 cells were treated with 10 μM Sar-acatinib or buffer and suspended for 3 h. Western blot probed with antibodies reactive to pTalin-S425, total Talin (Talin), HUTS-4 (ITGB1*), or total ITGB1/β1-integrin (ITGB1). **e-f** Re-adhesion of suspended DU145/shCDCP1 to fibronectin (**e**). Image of plate after adhesion

of DU145/shCDCP1 cells with and without treatment with Vanadate treatment and quantification of adherent cell numbers (**f**). Western blot tyrosine phosphorylated proteins visualized with the 4G10 antibody. *$P<0.05$ and **$P<0.01$
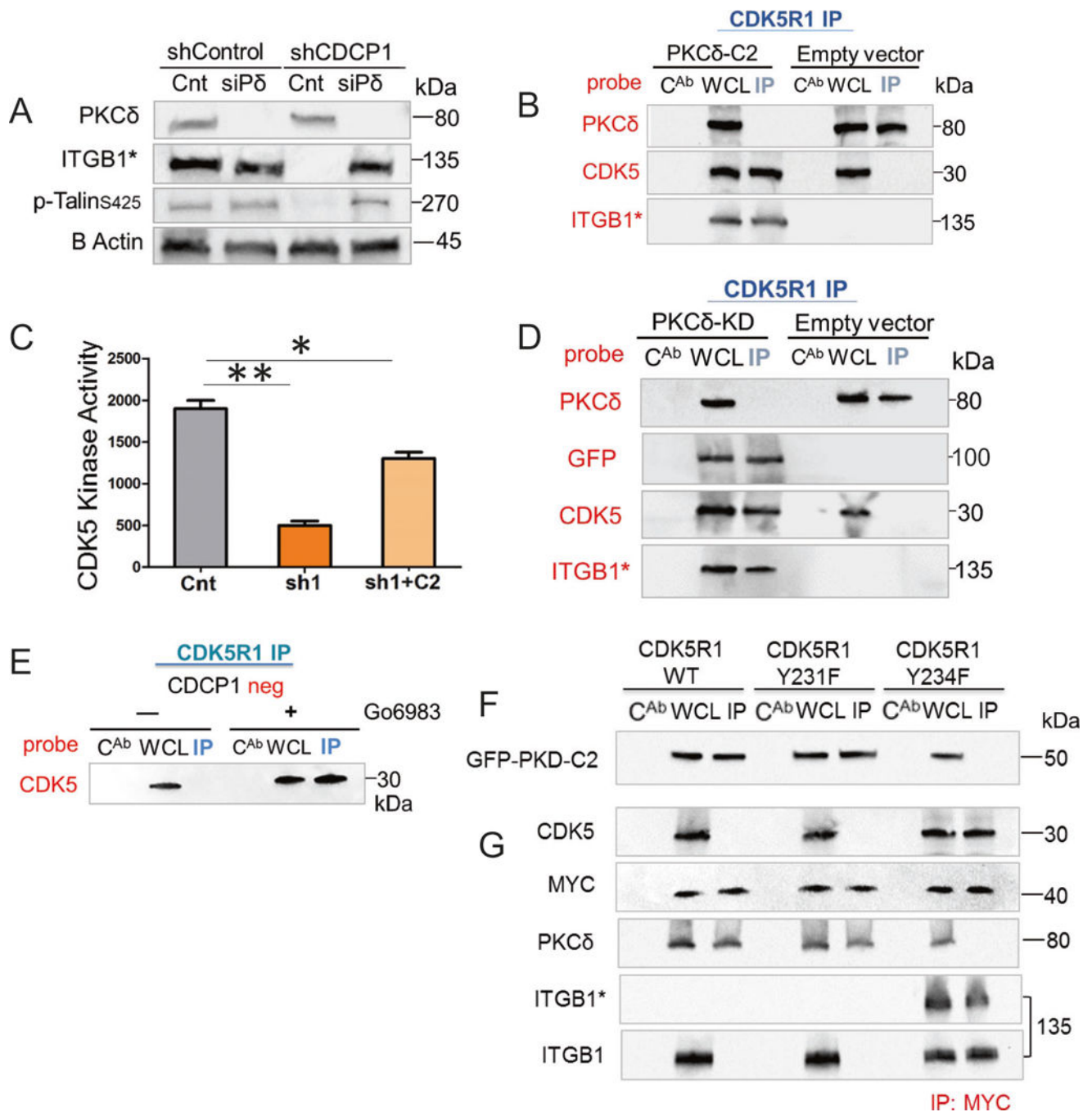
Fig. 6.

PKCδ binds phosphorylated CDK5R1/p35 via its C2 domain in CDCP1-silenced and suspended DU145 cells. **a** PKCδ (siPδ) silencing in suspended DU145/shCDCP1 leads to reactivation of ITGB1/β1-integrin. Equal amounts of whole lysates from DU145/shControl or DU145/shCDCP1 were analyzed by western blotting and probed with anti-PKCδ, HUTS-4 (ITGB1*), and anti-pTALIN. **b** Binding of GFPPKCδ-C2 domain to CDK5R1/p35. Western blots of CDK5R1 or IgG control (C^AB) immunopreceipitation of DU145/shCDCP1 expressing either GFP-PKCδ-C2 domain (PKCδ-C2) or empty vector. Membranes were

probed with antibodies reactive with PKCδ, CDK5, or HUTS-4. **c** Kinase assay of CDK5 in DU145 shControl (Cnt), shCDCP1 (sh1), and shCDCP1 + GFP-PKCδ-C2 overexpression (sh1 + C2). Kinase activity measured by incorporation of 32P into CDK5 substrate is plotted on the y-axis. **d** Overexpression of GFPtagged PKCδ kinase dead (PKCδ-KD) in DU145/ shCDCP1. Western blots of CDK5R1 immunoprecipitates (IP), whole cell lysate (WCL), or IgG control (C^{AB}) IPs from cells expressing GFP-PKCδ-KD or empty vector. Western blots were probed with antibodies detecting PKCδ, GFP, CDK5, or HUTS-4 (ITGB1*). **e** Inhibition of PKCδ with Go6983. The CDK5 and CDK5R1 complex formation is demonstrated with and without treatment with G06983. **f–g** pCDK5R1–PKCδ complex formation. **f** CDCP1-silenced cells were transfected with MYCtag-wt-CDK5R1, MYCtag-CDK5R1-Y231F, or MYCtag-CDK5R1-Y234F and co-transfected with GFP-PKCδ-C2 domain. Lysates were precipitated with the anti-MYCtag antibody and probed for GFP (**g**). Immunoprecipitation of cell expressing wild-type and mutant CDK5R1 as described in **f**. Membranes were probed with antibodies reactive with CDK5, MYC, PKCδ, HUTS-4 (ITGB1*) or total integrin (ITGB1). *$P < 0.05$ and **$P < 0.01$
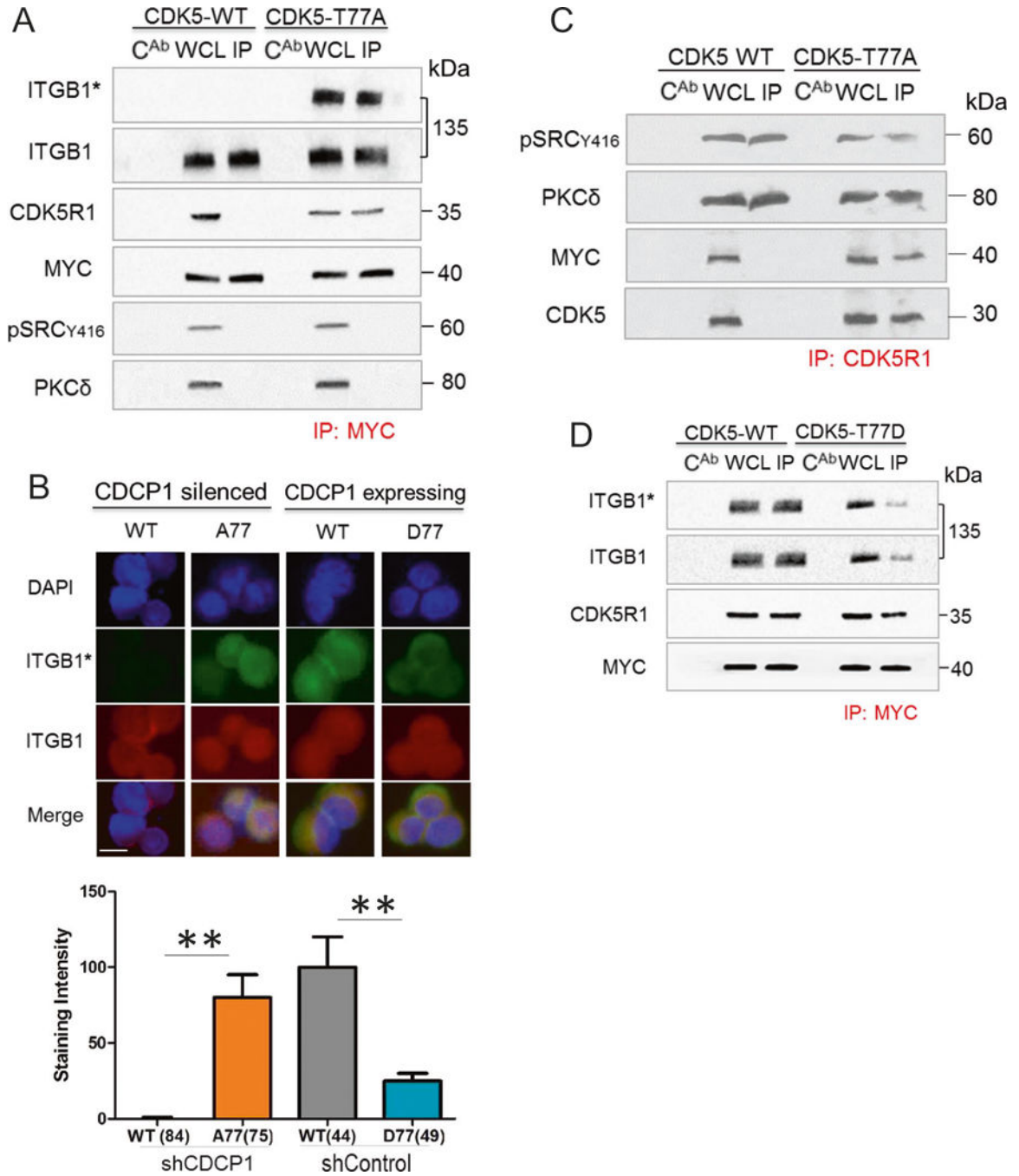
Fig. 7.
Phosphorylation of CDK5-T77 by PKC5 leads to dissociation of CDK5-CDKR1 complexes.
a CDK5-T77A complex formation. MYCtag-CDK5-T77A or MYCtag-wt-CDK5 were
expressed in suspended DU145/shCDCP1. Western blots of MYCtag- immunoprecipitations
(IP) and controls were probed with antibodies reactive with HUTS-4 (ITGB1*), total
ITGB1/β1-integrin (ITGB1), CDK5R1, or MYCtag. **b** CDCP1-silenced DU145 cells
transfected with wt-CDK5 (WT) and CDK5T77A (A77) or CDCP1-expressing DU145 cells
transfected with wt-CDK5 (WT) or CDK5T77D (D77) were probed for ITGB1* (green),

total integrin (red), or DAPI (blue). The staining was quantified using ImageJ. Staining intensities per cell are indicated on the y-axis. The number of cells analyzed is shown in parentheses. **c** CDK5–T77A complexes with CDK5R1. Western blot of CDK5R1 immunoprecipitation in DU145 cells described in **a**. Western blots were probed with antibodies reactive with pSRCY416, PKCδ, MYC, and CDK5. **d** CDK5–T77D complex formation. MYCtag-CDK5-T77D or MYCtag-wt-CDK5 were expressed in suspended DU145/shControl cells. Western blot as described in a. $*P < 0.05$ and $**P < 0.01$
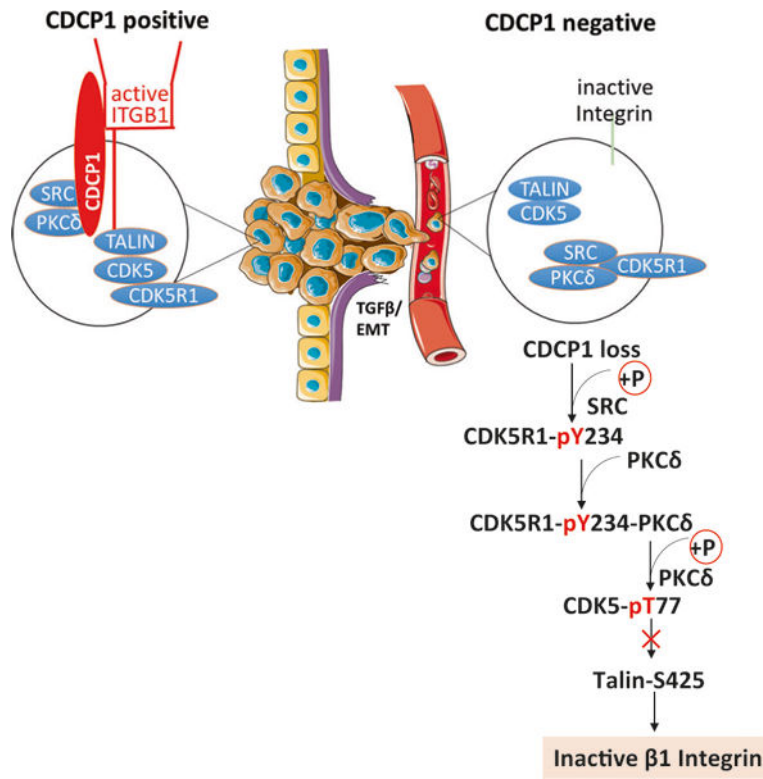
Fig. 8.
Model of loss of ITGB1/β1-integrin inside-out activation in detached prostate cancer cells with low CDCP1 expression